

湖州欢迎你！

1





2

相对论同量异位素核碰撞中的 核结构研究

徐浩洁

湖州师范学院

原子核结构与中高能重离子碰撞交叉学科理论讲习班，

湖州，2021年7月9-24日

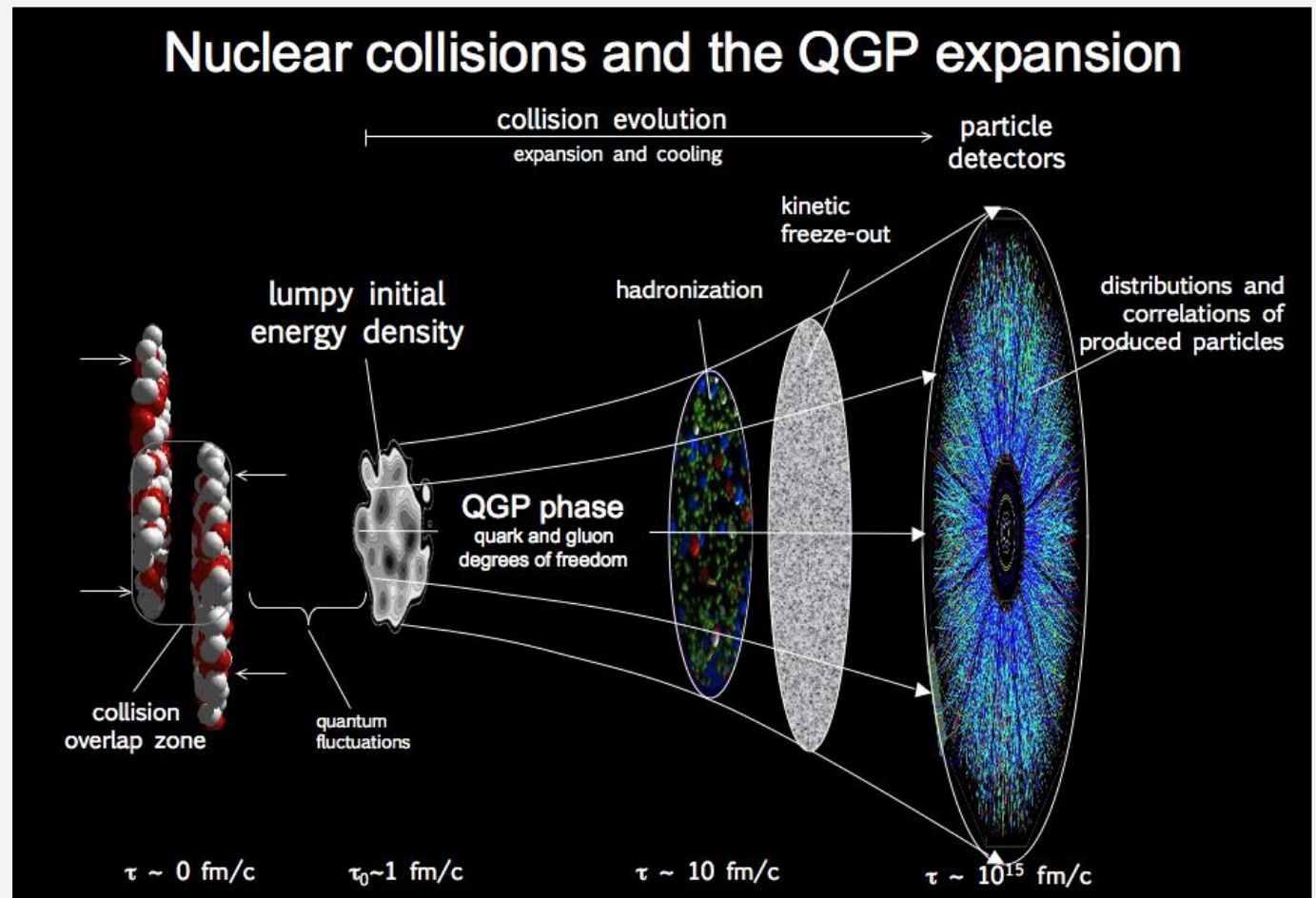
徐浩洁，湖州师范学院

提纲

- I. 相对论重离子碰撞简介
- II. 初态几何模型
- III. 核结构对手征磁效应测量的影响
- IV. 通过同量异位素核碰撞测量中子皮
- V. 总结

I. 相对论重离子碰撞简介

相对论重离子碰撞



相对论重离子碰撞的特点

- 极高的能量 (RHIC, $v=0.99995c$)
- 极短的碰撞时间 $fm/c \sim 10^{-23}s$
- 低重子数密度
- 极高温度 (QGP, 夸克胶子等离子体)
- 极强的磁场
- 极大的涡旋

相对论重离子碰撞的观测量

- 粒子产额（统计模型；反物质产生）
- 集体流（各向异性流及其关联；QGP性质）
- 电荷关联（手征磁效应等）
- 高阶矩（QCD相变）
- 电磁探针、重味探针、喷注淬火等等

相对论重离子碰撞的常用模型

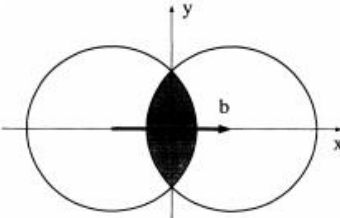
- 相对论流体力学模型
- AMPT模型
- UrQMD模型
- Hi jing模型
- ○ ○ ○ ○ ○

II. 初态几何模型



初始几何特性

- 非中心对撞几何不对称性



- 形变核

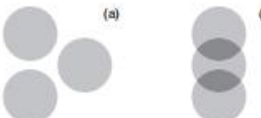


- 中子皮 (周边碰撞)

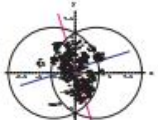


Hao-jie Xu et al., PLB-819(2021)136453,
Hanlin Li et al., PRL-125(2020)222301

- α -cluster 结构

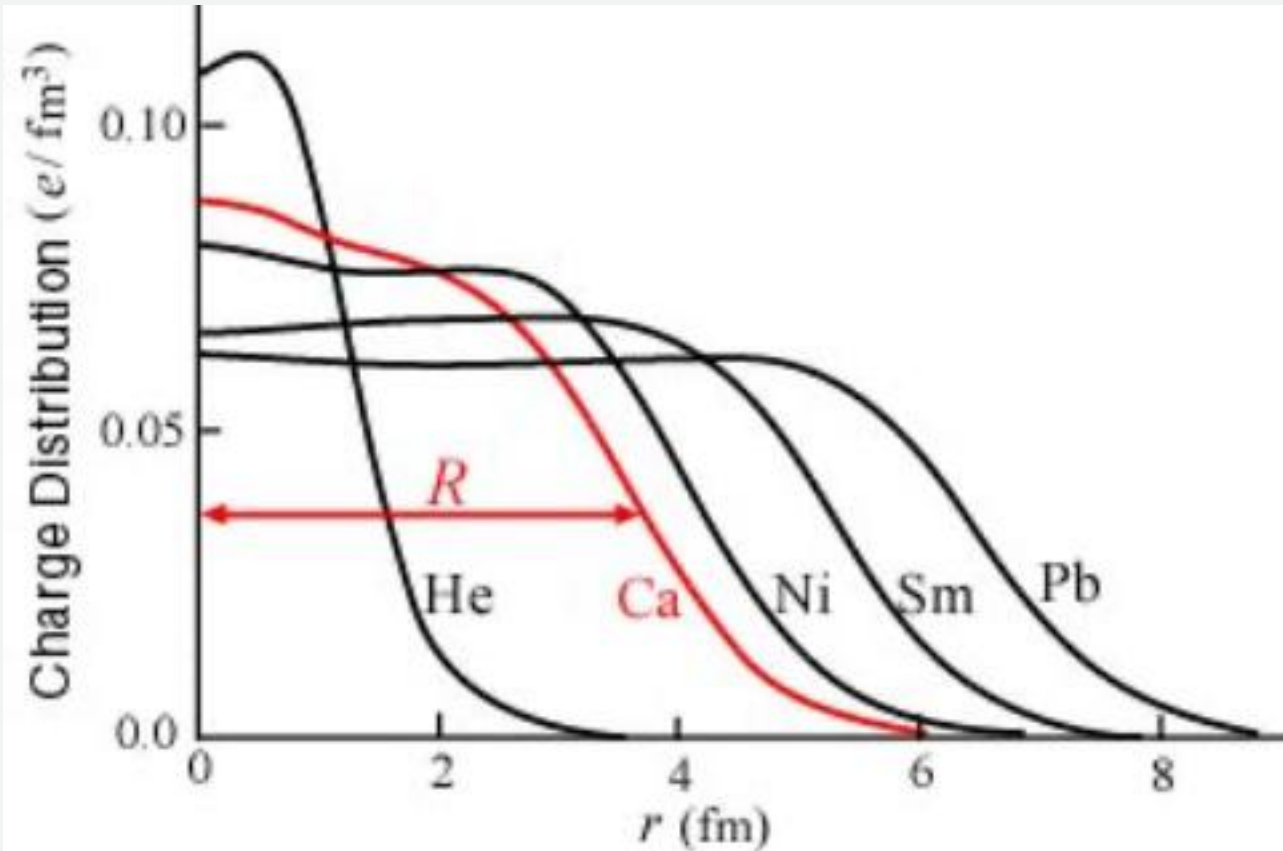


- 涨落



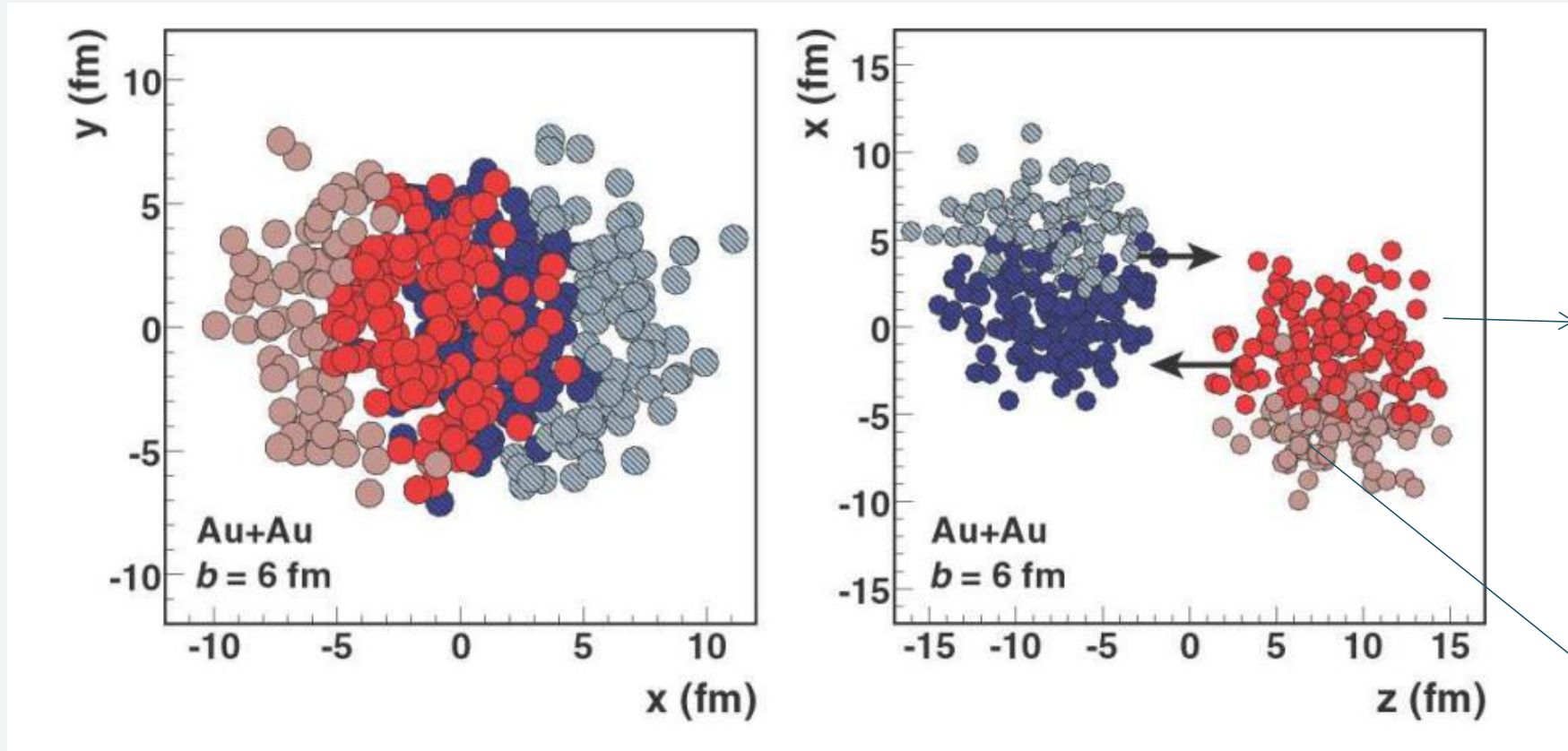
Woods-Saxon 分布

$$\rho(r) = \rho_0 \frac{1 + w \left(\frac{r}{R}\right)^2}{1 + e^{(r-R)/a}}$$



Nucleus	R [fm]	a [fm]	w [fm]
^2H	0.01	0.5882	0
^{16}O	2.608	0.513	-0.51
^{28}Si	3.34	0.580	-0.233
^{32}S	2.54	2.191	0.16
^{40}Ca	3.766	0.586	-0.161
^{58}Ni	4.309	0.517	-0.1308
^{62}Cu	4.2	0.596	0
^{186}W	6.58	0.480	0
^{197}Au	6.38	0.535	0
$^{207}\text{Pb}^a$	6.62	0.546	0
^{238}U	6.81	0.6	0

参与者与旁观者



Michael L. Miller, Klaus Reygers, Stephen J. Sanders, Peter Steinberg,
Ann.Rev.Nucl.Part.Sci. 57 (2007) 205-243

Optical Glauber model

- Thickness function

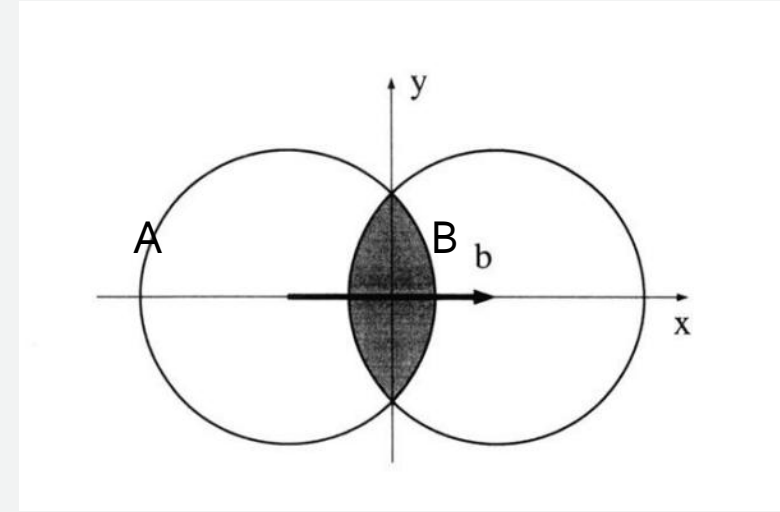
$$T(s_T) = \int_{-\infty}^{\infty} \rho(s_T, z) dz$$

- The probability of a nucleon in A interact with a nucleon in B is

$$p_{AB}(b) = \sigma_{in}^{NN} \frac{\int dx dy T_A(x + b/2, y) T_B(x - b/2, y)}{AB}$$

- For a given nucleon in A, it interact with a nucleon in B is

$$p_A(x, y; b) = \sigma_{in}^{NN} \frac{T_B(x - b/2, y)}{B}$$



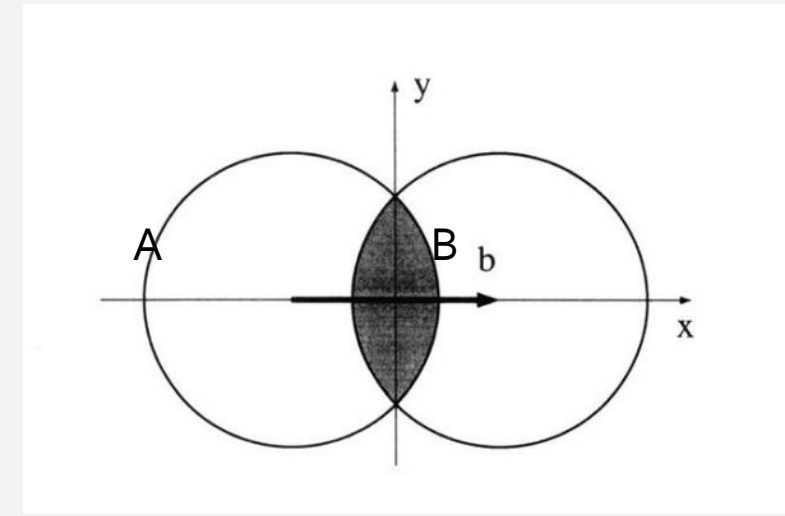
A+B cross section

- The probability of having n binary collision is

$$P(n) = \binom{AB}{n} p_{AB}^n (1 - p_{AB})^{AB-n}$$

- The total cross section of an interaction between A and B is

$$\begin{aligned}\frac{d^2\sigma_{in}^{A+B}}{db^2} &= \sum_{i=1}^{AB} P(n; b) = 1 - (1 - p_{AB})^{AB} \\ &\approx 1 - e^{-\sigma_{in}^{NN} \int dx dy T_A(x+b/2, y) T_B(x-b/2, y)}\end{aligned}$$



Number of binary collisions

$$N_{coll}(b) = \sum_{i=1}^{AB} nP(n; b) = \sigma_{in}^{NN} \int dx dy T_A(x + b/2, y) T_B(x - b/2, y)$$

Number of participant(wounded nucleons)

$$N_{part}(b) = \int dx dy T_A(x + b/2, y) \left\{ 1 - \left[1 - \sigma_{in}^{NN} \frac{T_B(x - b/2, y)}{B} \right]^B \right\} \\ + \int dx dy T_B(x - b/2, y) \left\{ 1 - \left[1 - \sigma_{in}^{NN} \frac{T_A(x + b/2, y)}{A} \right]^A \right\}$$

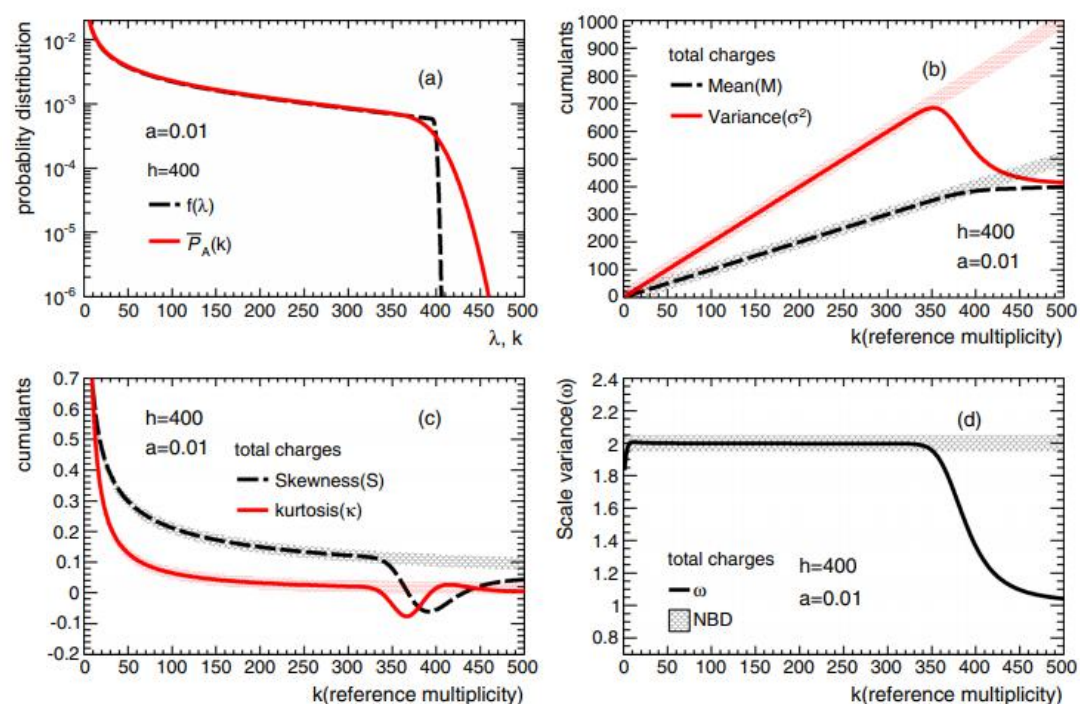
Cumulants of multiplicity distributions in most-central heavy-ion collisions

Hao-jie Xu^{*}

Department of Physics and State Key Laboratory of Nuclear Physics and Technology, Peking University, Beijing 100871, China

(Received 17 April 2016; revised manuscript received 11 August 2016; published 11 November 2016)

I investigate the volume corrections on cumulants of total charge distributions and net proton distributions. The required volume information is generated by an optical Glauber model. I find that the corrected statistical expectations of multiplicity distributions mimic the negative binomial distributions at noncentral collisions, and they tend to approach the Poisson ones at most-central collisions. The volume corrections are due to the external volume fluctuations at most-central collisions. The volume distributions in event-by-event multiplicity fluctuation



优点：解析公式，不占计算资源

缺点：没有涨落

涨落

Glauber modeling in high energy nuclear collisions

Michael L. Miller (MIT, LNS), Klaus Reygers (Munster U.), Stephen J. Sanders (Kansas U.), Peter Steinberg (Brookhaven) (Jan, 2007)

Published in: *Ann.Rev.Nucl.Part.Sci.* 57 (2007) 205-243 • e-Print: nucl-ex/0701025 [nucl-ex]

[pdf](#) [DOI](#) [cite](#)

#1

1,467 citations

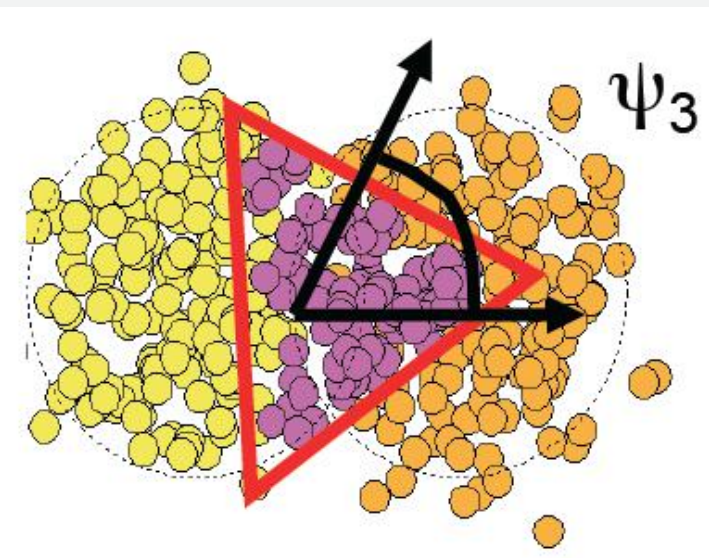
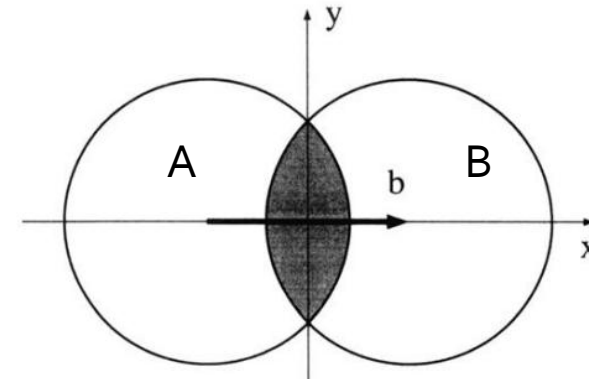
The PHOBOS Glauber Monte Carlo

B. Alver (MIT), M. Baker (Brookhaven), C. Loizides (MIT), P. Steinberg (Brookhaven) (May, 2008)

e-Print: 0805.4411 [nucl-ex]

[pdf](#) [cite](#)

#3



The effect of triangular flow on di-hadron azimuthal correlations in relativistic heavy ion collisions

Jun Xu (Texas A-M), Che Ming Ko (Texas A-M, Cyclotron Inst. and Texas A-M) (Nov, 2010)

Published in: *Phys.Rev.C* 83 (2011) 021903 • e-Print: 1011.3750 [nucl-th]

[pdf](#) [DOI](#) [cite](#)

#1

59 citations

Elliptic and triangular flow in event-by-event (3+1)D viscous hydrodynamics

Bjorn Schenke (McGill U.), Sangyong Jeon (McGill U.), Charles Gale (McGill U.) (Sep, 2010)

Published in: *Phys.Rev.Lett.* 106 (2011) 042301 • e-Print: 1009.3244 [hep-ph]

[pdf](#) [DOI](#) [cite](#)

#2

611 citations

Triangular flow in event-by-event ideal hydrodynamics in Au+Au collisions at $\sqrt{s_{NN}} = 200A$ GeV

Hannah Petersen (Duke U.), Guang-You Qin (Duke U.), Steffen A. Bass (Duke U.), Berndt Muller (Duke U.) (Aug, 2010)

Published in: *Phys.Rev.C* 82 (2010) 041901 • e-Print: 1008.0625 [nucl-th]

[pdf](#) [DOI](#) [cite](#)

#3

202 citations

Triangular flow in hydrodynamics and transport theory

Burak Han Alver (MIT, LNS), Clement Gombeaud (Saclay, SPhT), Matthew Luzum (Saclay, SPhT), Jean-Yves Ollitrault (Saclay, SPhT) (Jul, 2010)

Published in: *Phys.Rev.C* 82 (2010) 034913 • e-Print: 1007.5469 [nucl-th]

[pdf](#) [DOI](#) [cite](#)

#4

345 citations

Collision geometry fluctuations and triangular flow in heavy-ion collisions

B. Alver (MIT), G. Roland (MIT) (Mar, 2010)

Published in: *Phys.Rev.C* 81 (2010) 054905, *Phys.Rev.C* 82 (2010) 039903 (erratum) • e-Print: 1003.0194 [nucl-th]

[pdf](#) [DOI](#) [cite](#)

#5

807 citations

蒙特卡洛Glauber模型的一些细节

- 如何判断碰撞发生

Step function

$$d \leq \sqrt{\sigma_{\text{inel}}^{\text{NN}}/\pi}$$

Gaussian function

$$p(b) = Ae^{-\pi Ab^2/\sigma_{\text{inel}}}.$$

- Recenter(1)

PHYSICAL REVIEW C 84, 064913 (2011)

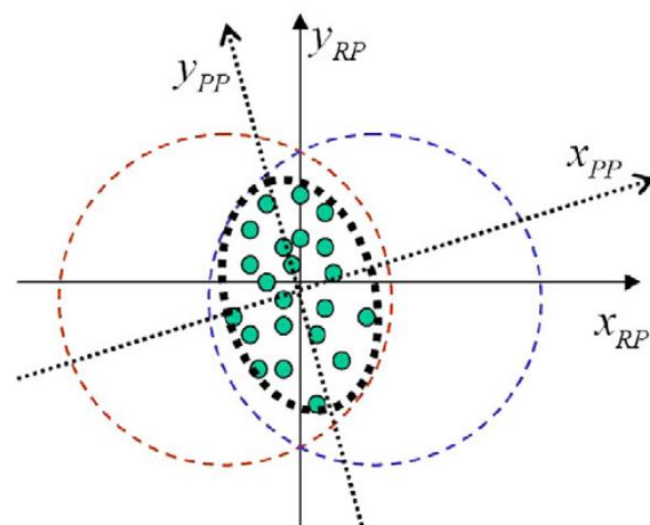
Wounded-nucleon model with realistic nucleon-nucleon collision profile and observables in relativistic heavy-ion collisions

Maciej Rybczyński^{1,*} and Wojciech Broniowski^{2,†}

¹Institute of Physics, Jan Kochanowski University, PL-25406 Kielce, Poland

²The H. Niewodniczański Institute of Nuclear Physics, Polish Academy of Sciences, PL-31342 Kraków, Poland

(Received 1 September 2011; published 22 December 2011)



Eccentricity (Point-like nucleons)

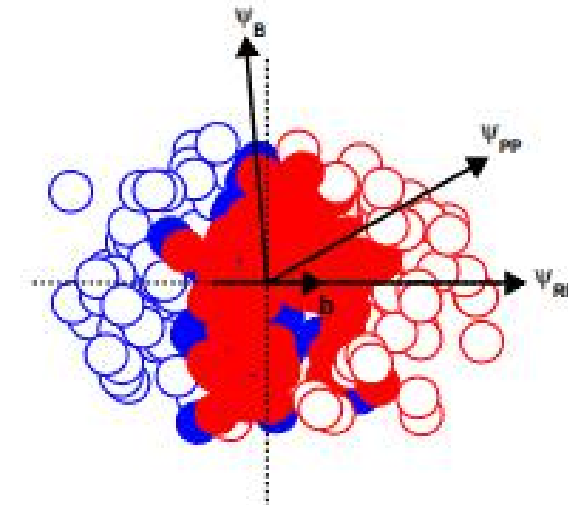
$$\psi_n\{\text{part}\} = \frac{1}{n} \left[\arctan \frac{\langle r^n \sin(n\varphi) \rangle}{\langle r^n \cos(n\varphi) \rangle} + \pi \right] \quad \text{Recenter(2)}$$

$$\varepsilon_n\{\text{part}\} = \frac{\sqrt{\langle r^n \cos(n\varphi) \rangle^2 + \langle r^n \sin(n\varphi) \rangle^2}}{\langle r^n \rangle},$$

$$\varepsilon_n(b), \varepsilon_n(N_{part})$$

$$\varepsilon_n(N_{ch}),$$

$$N_{ch} = n_{pp}(xN_{coll} + (1-x)N_{part}/2)$$



Energy (entropy) density

Two-component Glauber

$$\begin{aligned}s_0(\mathbf{x}_\perp) &= \frac{dS}{\tau_0 dx dy d\eta_s} \Big|_{\eta_s=0} \\ &= \frac{C}{\tau_0} \left(\frac{1-\delta}{2} \frac{dN_{\text{part}}}{d^2 x_\perp} + \delta \frac{dN_{\text{coll}}}{d^2 x_\perp} \right).\end{aligned}$$

Color Glass condensate (CGC)

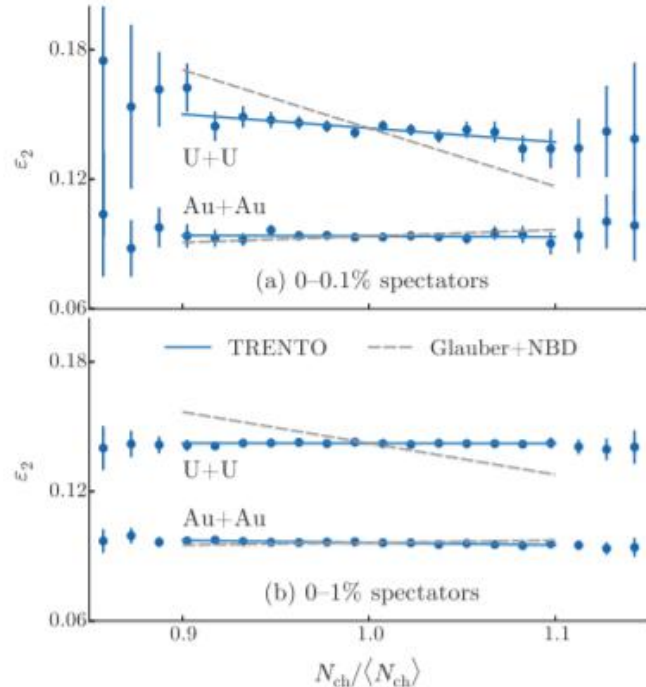
$$\begin{aligned}s_0(\mathbf{x}_\perp) &= 3.6 n_g \\ &= 3.6 \frac{dN_g}{\tau_0 d^2 x_\perp d\eta_s} \Big|_{y=\eta_s=0}.\end{aligned}$$

$$\begin{aligned}\frac{dN_g}{d^2 x_\perp dy} &= \frac{2\pi^2}{C_F} \int \frac{d^2 p_T}{p_T^2} \int^{p_T} \frac{d^2 k_T}{4} \alpha_s(Q^2) \\ &\times \phi_A(x_1, (\mathbf{p}_T + \mathbf{k}_T)^2/4; \mathbf{x}_\perp) \\ &\times \phi_B(x_2, (\mathbf{p}_T - \mathbf{k}_T)^2/4; \mathbf{x}_\perp),\end{aligned}$$

$$Q_{s,A}^2(x; \mathbf{x}_\perp) = Q_{s,0}^2 \frac{T_A(\mathbf{x}_\perp)}{T_{A,0}} \left(\frac{x_0}{x} \right)^\lambda$$

Energy (entropy) density

Trento model



Alternative ansatz to wounded nucleon and binary collision scaling in high-energy nuclear collisions

J. Scott Moreland, Jonah E. Bernhard, and Steffen A. Bass

Department of Physics, Duke University, Durham, North Carolina 27708-0305, USA

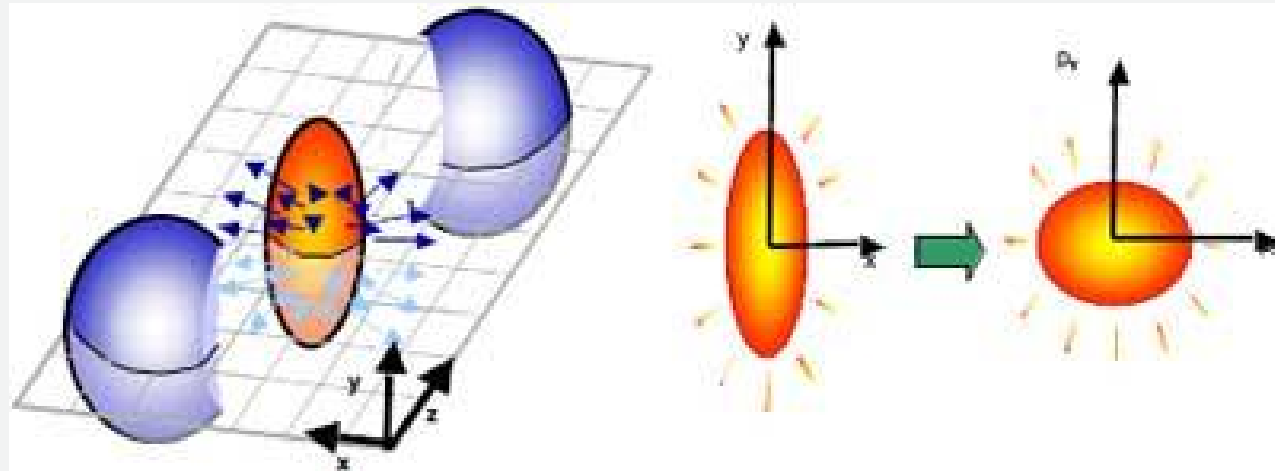
(Received 23 December 2014; revised manuscript received 11 May 2015; published 6 July 2015)

We introduce a new parametric initial-condition model for high-energy nuclear collisions based on eikonal entropy deposition via a “reduced-thickness” function. The model simultaneously describes experimental proton-proton, proton-nucleus, and nucleus-nucleus multiplicity distributions and generates nucleus-nucleus eccentricity harmonics consistent with experimental flow constraints. In addition, the model is compatible with ultracentral uranium-uranium data unlike existing models that include binary collision terms.

$$f = T_R(p; T_A, T_B) \equiv \left(\frac{T_A^p + T_B^p}{2} \right)^{1/p},$$

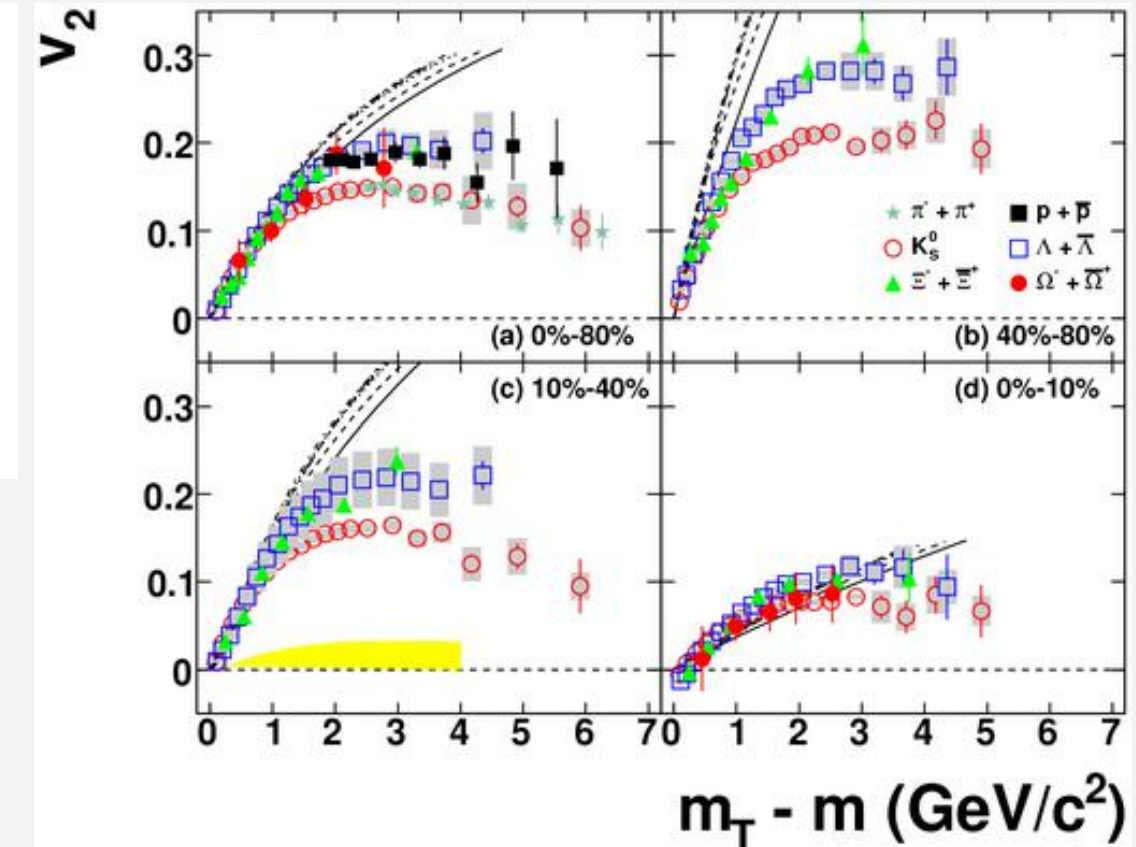
$$T_R = \begin{cases} \max(T_A, T_B), & p \rightarrow +\infty \\ (T_A + T_B)/2, & p = +1 \text{ (arithmetic)} \\ \sqrt{T_A T_B}, & p = 0 \text{ (geometric)} \\ 2T_A T_B/(T_A + T_B), & p = -1 \text{ (harmonic)} \\ \min(T_A, T_B), & p \rightarrow -\infty. \end{cases}$$

Collision geometry and anisotropic flow



With the WS densities, we have made very successful connections between the **final flow observable** and the **initial collision geometry**.

Prefect fluid - strong coupling QGP (sQGP)



$$\frac{dN}{d\phi} = N(1 + 2 \sum_n v_n \cos [n(\phi - \Psi_n)])$$

STAR, PRC 77, 054901 (2018)

Flow analysis with cumulants: Direct calculations

Ante Bilandzic,^{1,2} Raimond Snellings,² and Sergei Voloshin³

¹*Nikhef, Science Park 105, NL-1098 XG Amsterdam, The Netherlands*

²*Utrecht University, P.O. Box 80000, NL-3508 TA Utrecht, The Netherlands*

³*Wayne State University, 666 West Hancock Street, Detroit, Michigan 48201, USA*

(Received 6 October 2010; published 26 April 2011)

Anisotropic flow measurements in heavy-ion collisions provide important information on the properties of hot and dense matter. These measurements are based on analysis of azimuthal correlations and might be biased by contributions from correlations that are not related to the initial geometry, so-called nonflow. To improve anisotropic flow measurements, advanced methods based on multiparticle correlations (cumulants) have been developed to suppress nonflow contribution. These multiparticle correlations can be calculated by looping over all possible multiplets, however, this quickly becomes prohibitively CPU intensive. Therefore, the most used technique for cumulant calculations is based on generating functions. This method involves approximations, and has its own biases, which complicates the interpretation of the results. In this paper we present a new exact method for direct calculations of multiparticle cumulants using moments of the flow vectors.

$$Q_n \equiv \sum_{i=1}^M e^{in\phi_i},$$

$$\langle 2 \rangle = \frac{|Q_n|^2 - M}{M(M-1)}.$$

$$\begin{aligned} \langle 4 \rangle &= \frac{|Q_n|^4 + |Q_{2n}|^2 - 2 \cdot \text{Re}[Q_{2n} Q_n^* Q_n^*]}{M(M-1)(M-2)(M-3)} \\ &\quad - 2 \frac{2(M-2) \cdot |Q_n|^2 - M(M-3)}{M(M-1)(M-2)(M-3)}. \end{aligned}$$

Hydrodynamics and flow

$$\partial_\mu T^{\mu\nu}(x) = 0 \quad \text{and} \quad \partial_\mu j^\mu(x) = 0,$$



ELSEVIER

22 March 2001

Physics Letters B 503 (2001) 58–64

PHYSICS LETTERS B

www.elsevier.nl/locate/npe

Radial and elliptic flow at RHIC: further predictions

P. Huovinen^a, P.F. Kolb^{b,c}, U. Heinz^b, P.V. Ruuskanen^d, S.A. Voloshin^e

^a Lawrence Berkeley National Laboratory, Berkeley, CA 94720, USA

^b Department of Physics, The Ohio State University, 174 West 18th Avenue, Columbus, OH 43210, USA

^c Institut für Theoretische Physik, Universität Regensburg, D-93040 Regensburg, Germany

^d Department of Physics, University of Jyväskylä, FIN-40341 Jyväskylä, Finland

^e Department of Physics and Astronomy, Wayne State University, 666 W. Hancock Street, Detroit, MI 48202, USA

Received 12 January 2001; accepted 30 January 2001

Editor: R. Gatto

徐浩洁，湖州师范学院

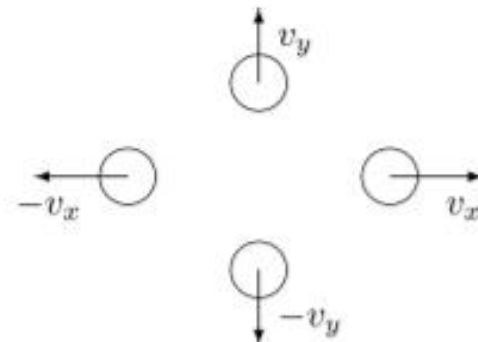


Fig. 6. Simple source of four fireballs.

$$v_2(p_t) \approx \tanh\left(\frac{1}{2}\left(\frac{\kappa p_t - \lambda m_t}{T} + \mu\right)\right),$$

flow fluctuation & correlations

Collective flow in 2.76 A TeV and 5.02 A TeV Pb+Pb collisions

#14

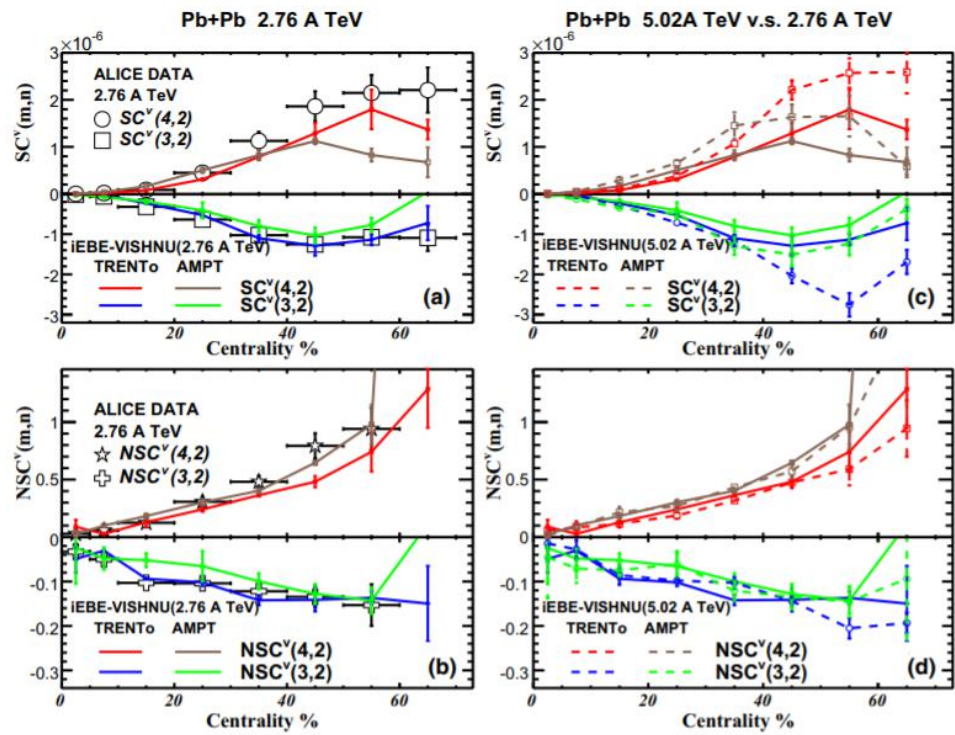
Wenbin Zhao (Peking U. and Peking U., SKLNPT), Hao-jie Xu (Peking U. and Peking U., SKLNPT), Huichao Song (CICQM, Beijing and Peking U., CHEP and Peking U., SKLNPT) (Mar 31, 2017)

Published in: *Eur.Phys.J.C* 77 (2017) 9, 645 • e-Print: 1703.10792 [nucl-th]

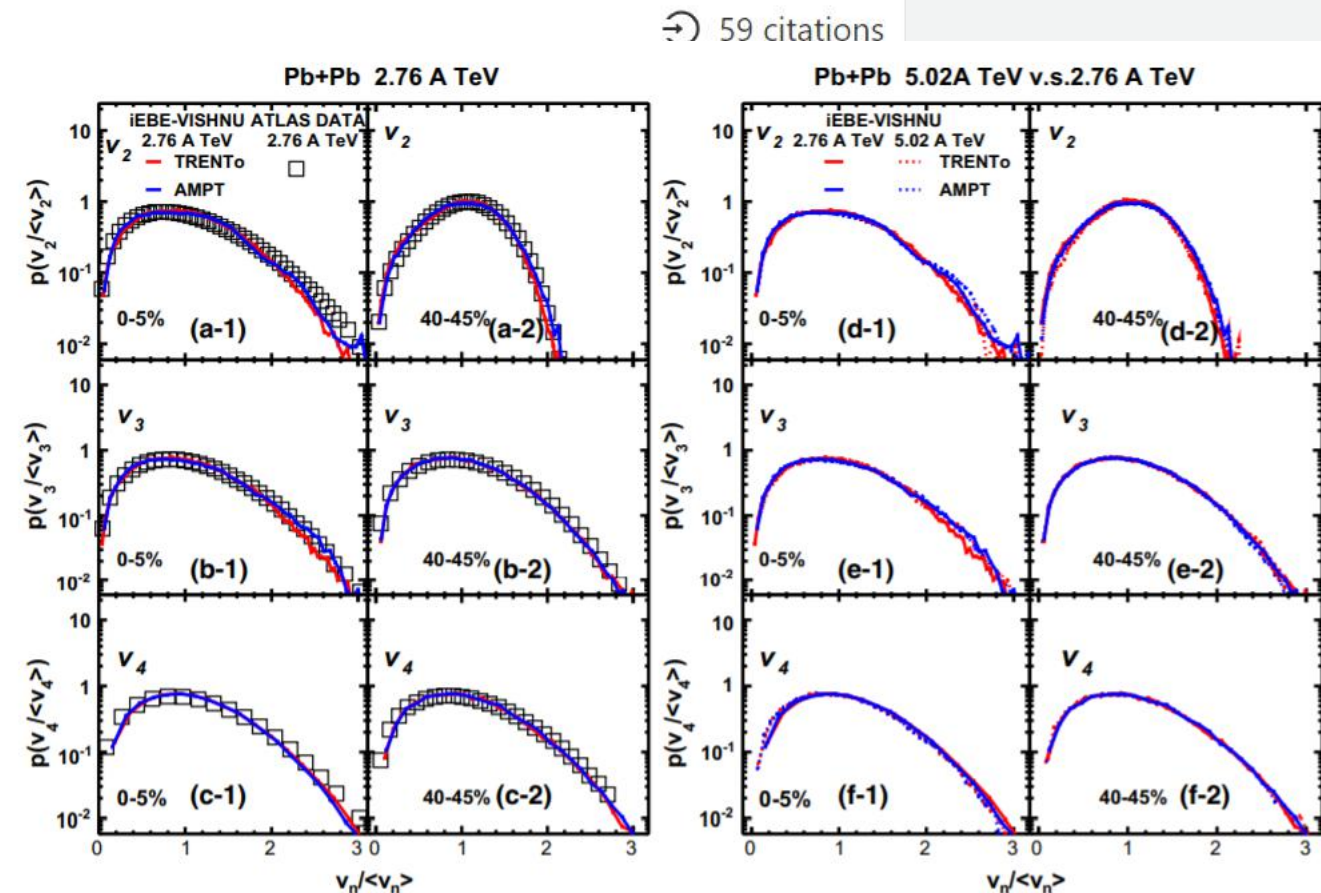
pdf

DOI

cite



徐浩洁, 湖州师范学院



25

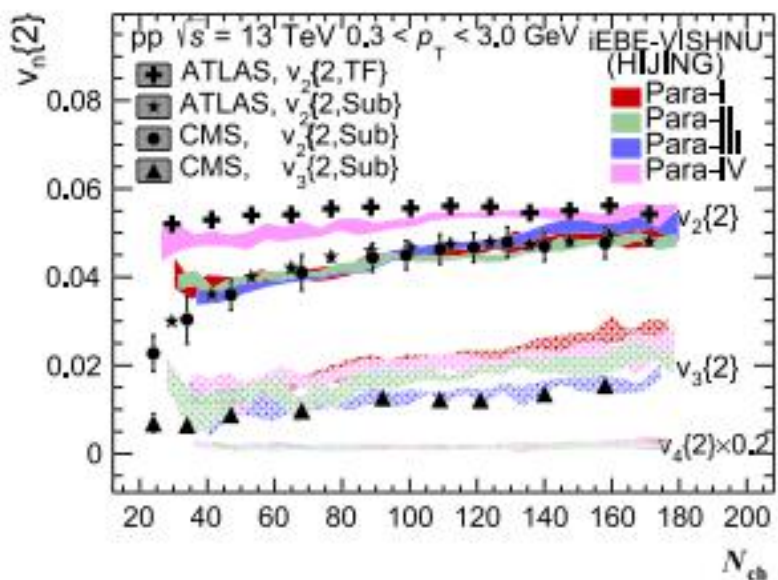


flow fluctuation in small system

Table 1

Four sets parameters used in iEBE-VISHNU simulations with HIJING initial conditions for pp collisions at 13 TeV.

	σ_R	σ_0	t_0	η/s	K	T_{sw} (MeV)
Para-I	1.0	0.4	0.1	0.07	126	147
Para-II	0.8	0.4	0.2	0.08	125	148
Para-III	0.4	0.2	0.6	0.20	113	148
Para-IV	0.6	0.4	0.4	0.05	128	147



徐浩洁，湖州师范学院



ELSEVIER

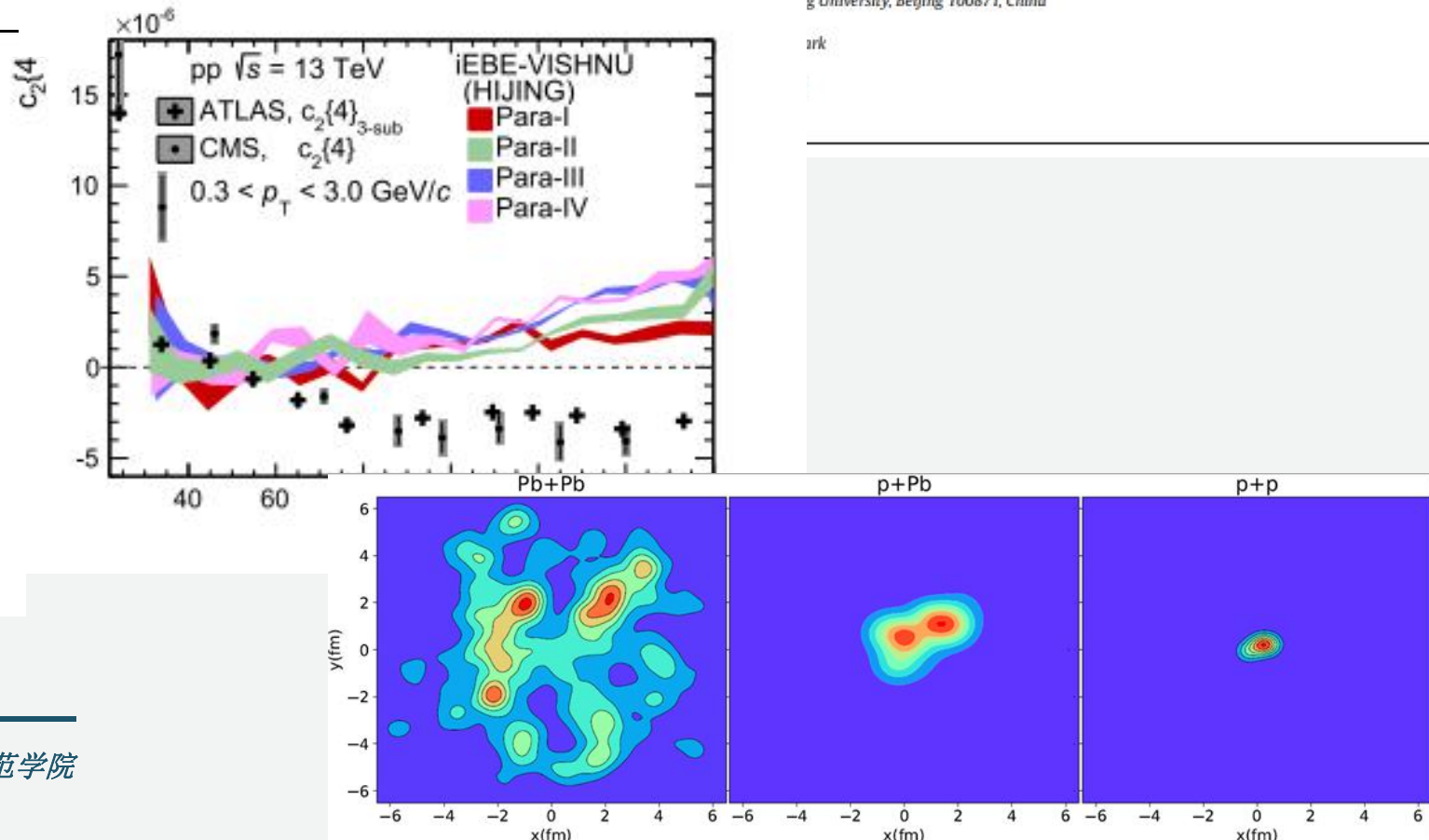
Hydrodynamic collectivity in proton-proton collisions at 13 TeV

Wenbin Zhao ^{a,b}, You Zhou ^{c,*}, Hao-jie Xu ^{d,a}, Weitian Deng ^e, Huichao Song ^{a,b,f,*}



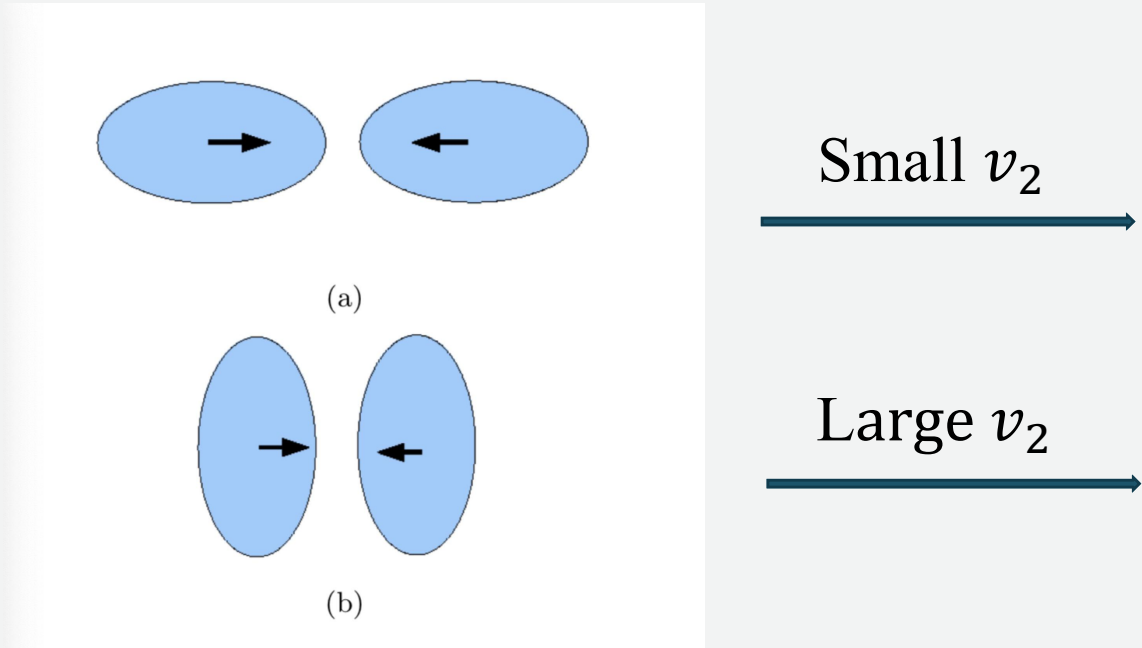
^a University, Beijing 100871, China

ark



Effect of deformation

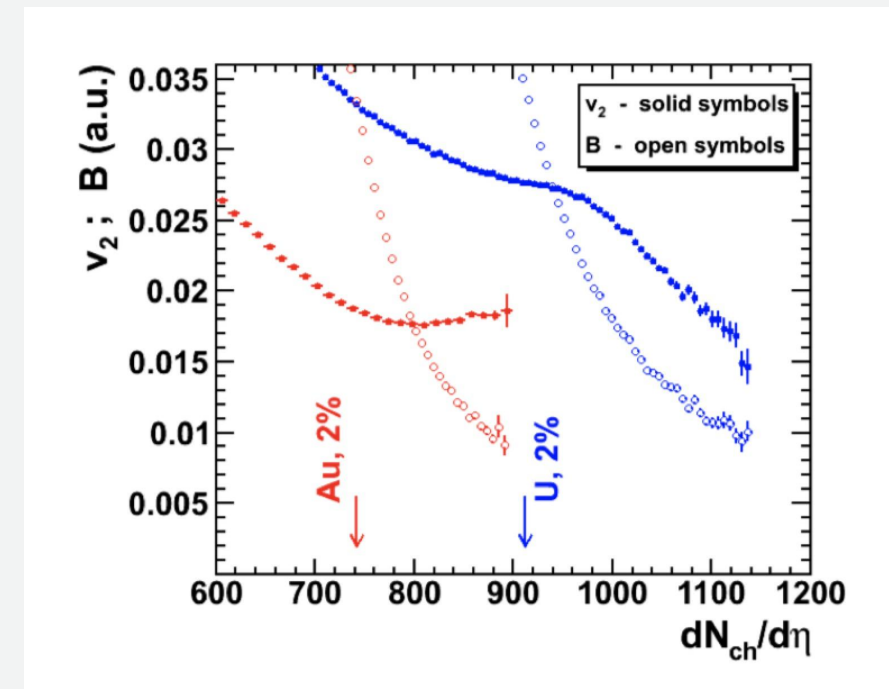
$$\rho(r) = \frac{\rho_0}{1 + \exp\left[\frac{r - R(1 + \beta_2 Y_{20} + \beta_4 Y_{40})}{a}\right]}$$



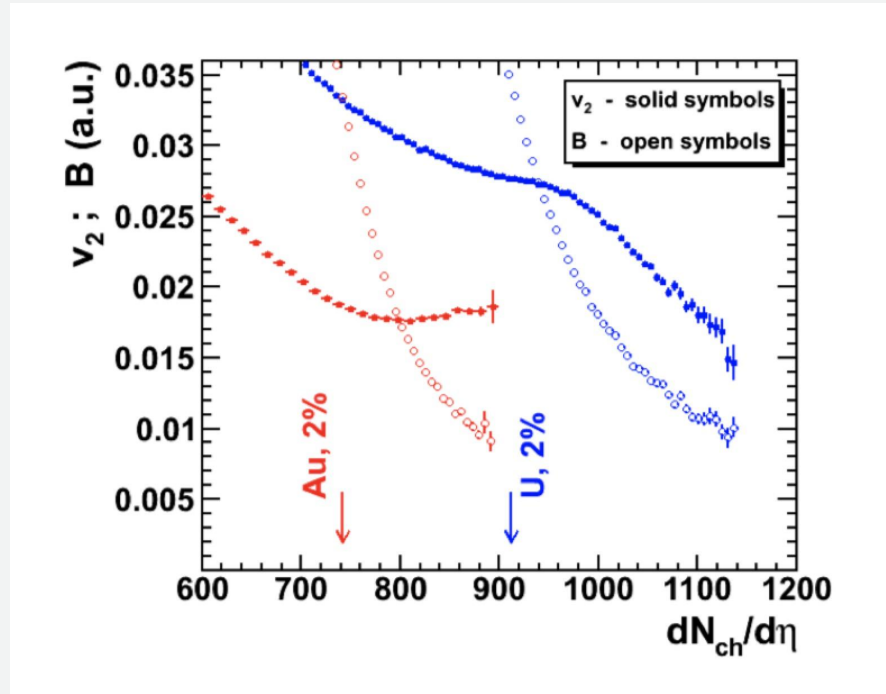
S. Voloshin, PRL105, 172301 (2010)

Au: $\beta_2 = -0.131$; U: $\beta_2 = 0.28$

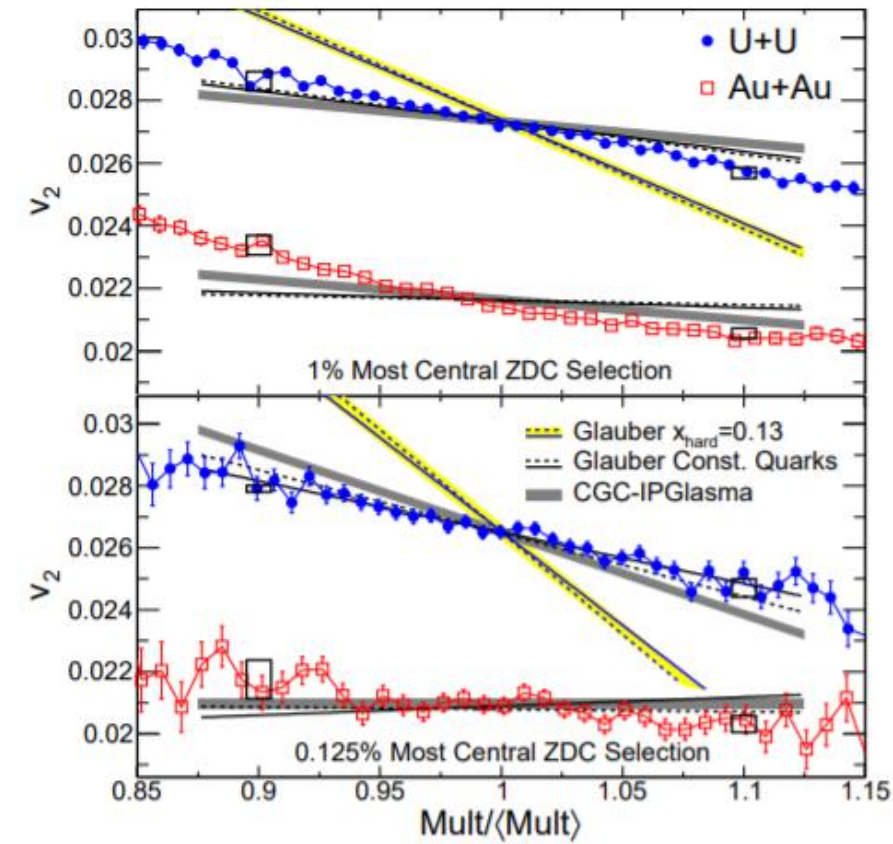
Knee structure of v_2 distributions at most-central U+U collisions



From Glauber to Trento

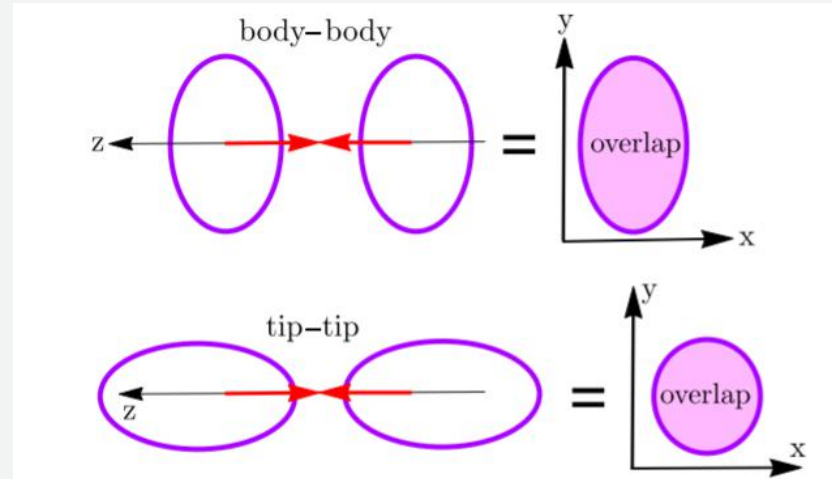
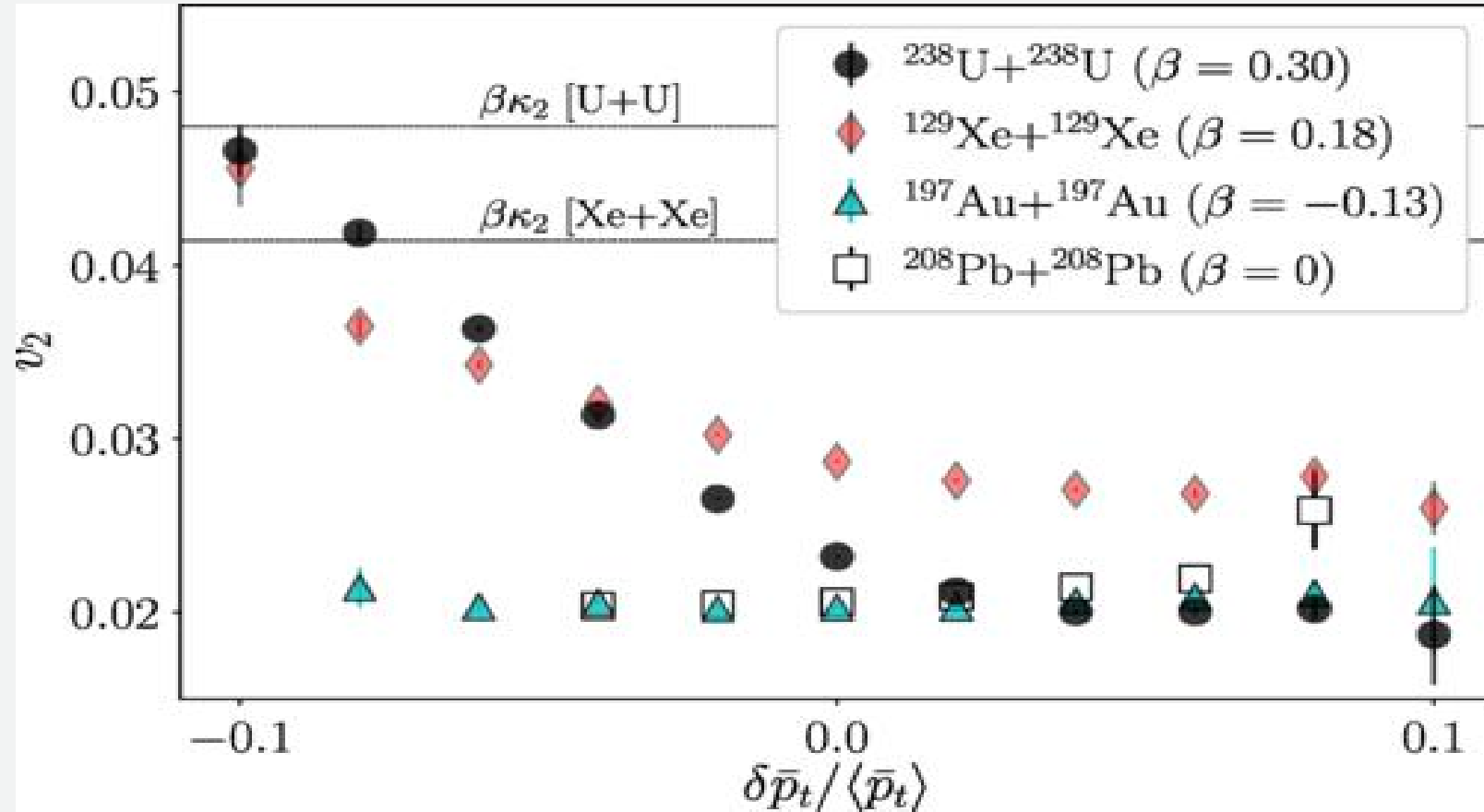


S. Voloshin, PRL105, 172301 (2010)



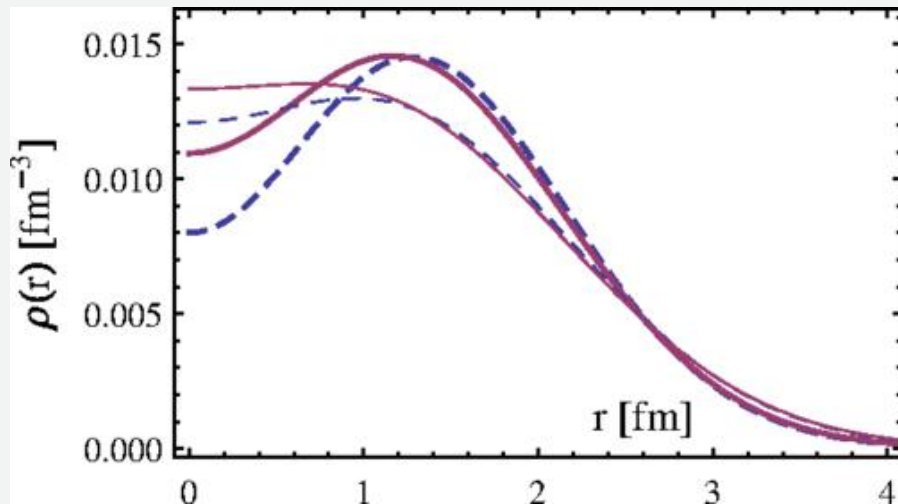
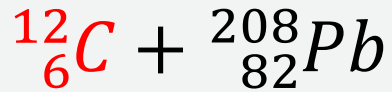
STAR, PRL115, 222301 (2015)

Prediction with Trento



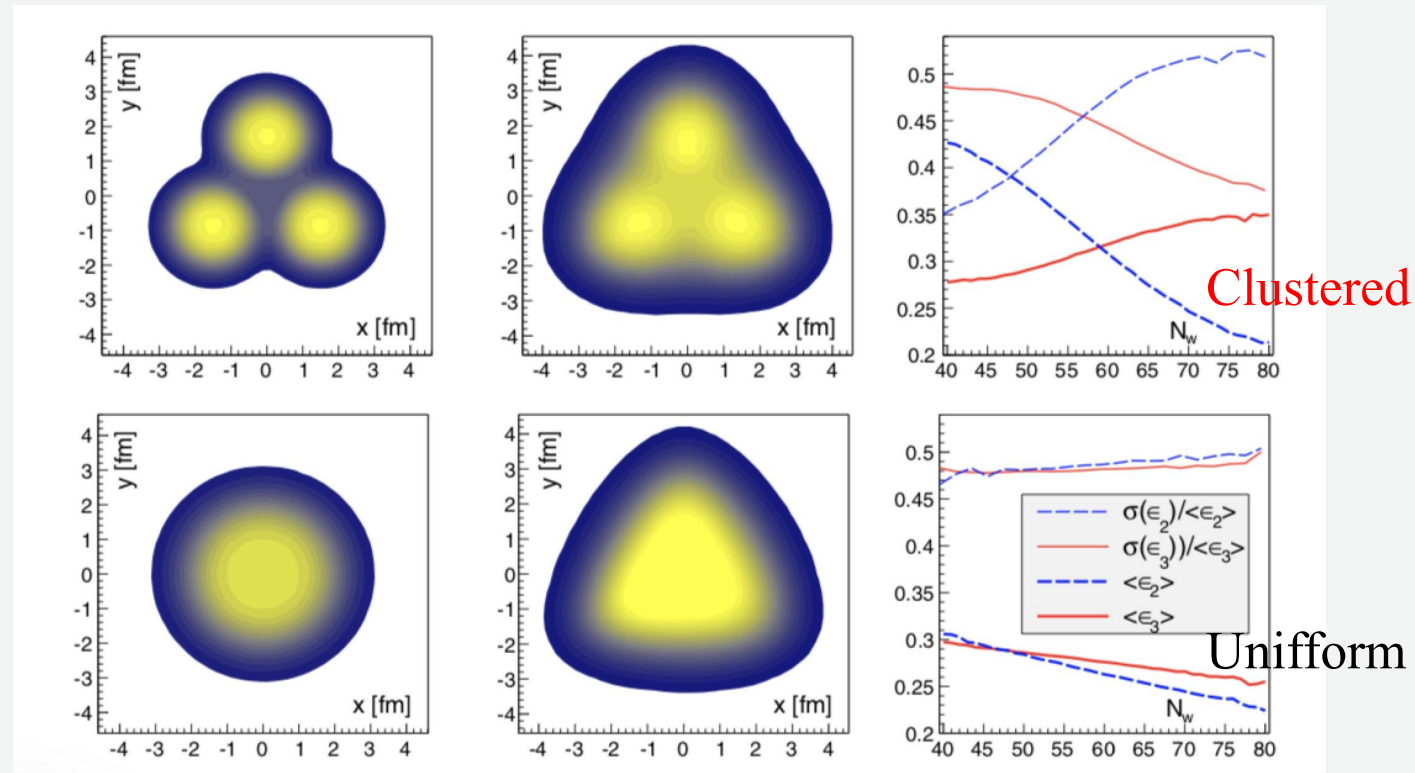
G. Giacalone, PRL124, 202301 (2020)

Effect of cluster correlations



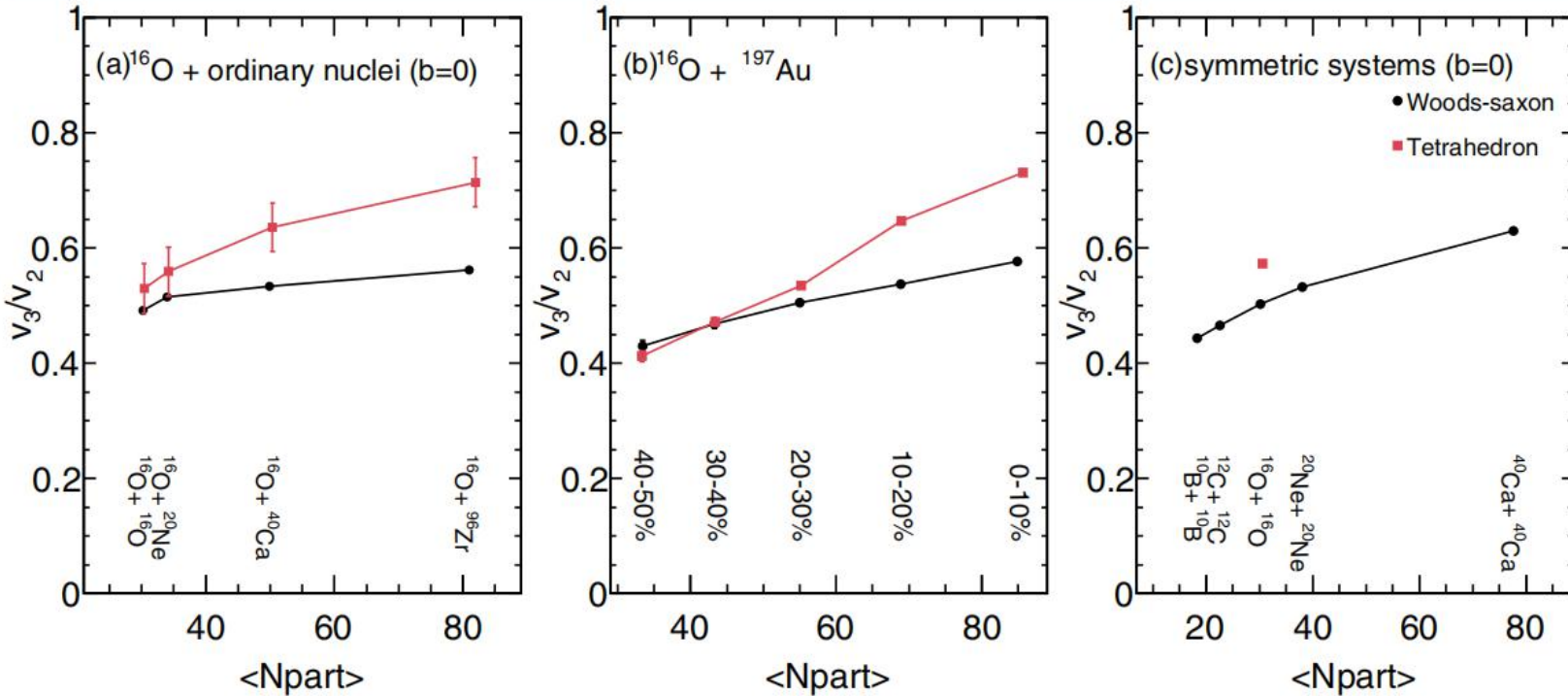
W. Broniowski, E. Arriola, PRL112,
112501 (2014)

徐浩洁, 湖州师范学院



The α -clustered and uniform ^{12}C have very different predictions on v3, its event-by-event fluctuations, or the correlations of the v2 and v3

利用系统扫描甄别 α -cluster结构



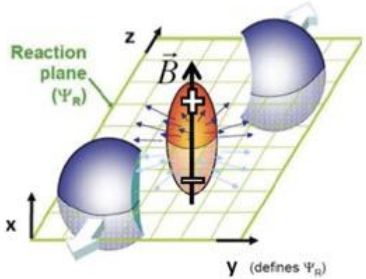
- ✓ 非对称系统扫描， v_3/v_2 两种构型具有明显的差别，WS构型非常平坦
- ✓ $^{16}\text{O} + ^{197}\text{Au}$ 中心度依赖，高多重数下 v_3/v_2 的比，两种构型具有明显的差别
- ✓ 对称系统扫描，明显看到四面体构型的 $^{16}\text{O} + ^{16}\text{O}$ 系统的 v_3/v_2 偏离系统学

Y.A. Li, S. Zhang, Y.G. Ma, Phys. Rev. C 102, 054907 (2020)

Isobar collisions

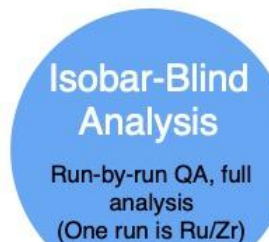
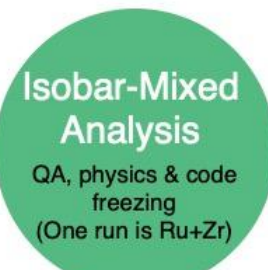
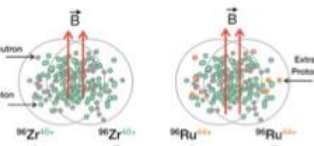


Chiral Magnetic Effect (CME)



- CME: a novel phenomenon predicted in HI collisions
 - Prerequisite: chiral imbalance+ magnetic field
 - Consequence: charge separation along B field
- **Experimental search is challenging due to overwhelming background → Isobar**

Isobar Blind Analysis



STAR, arXiv:1911.00596
Cartoon: arXiv:2009.01230

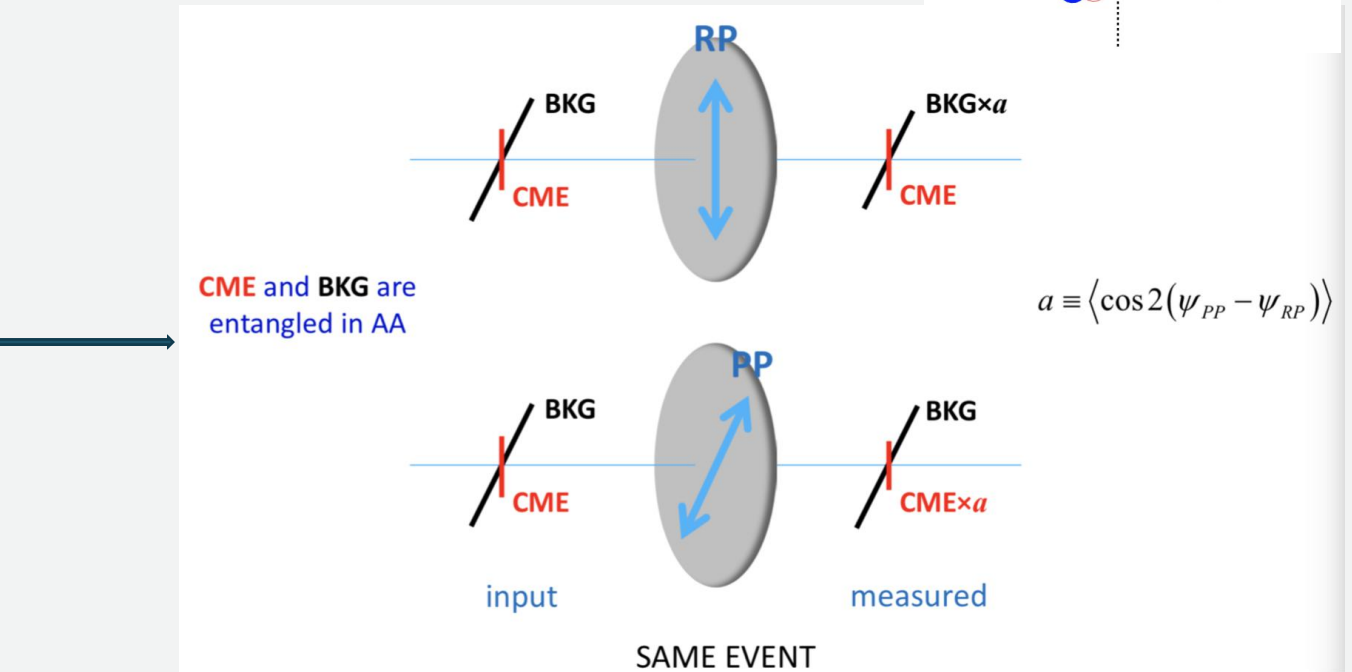
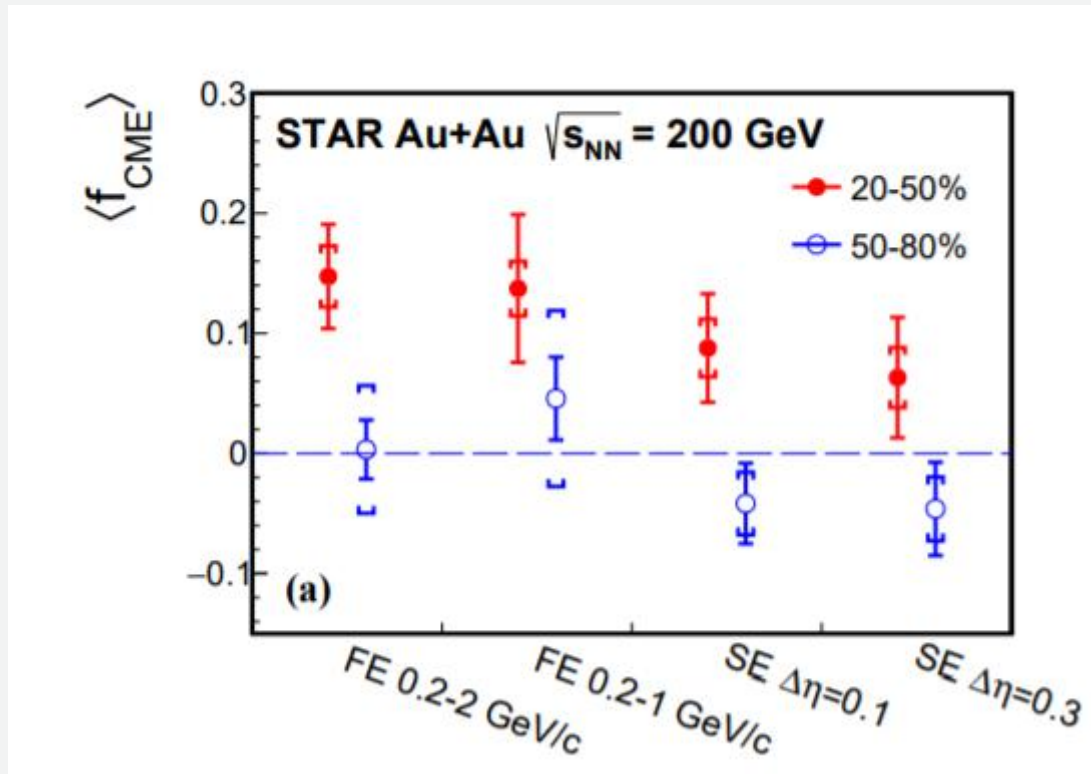
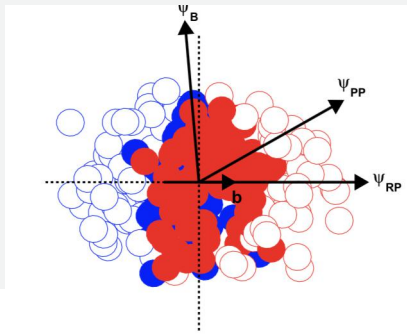
Processing...

05/17/2021

Rongrong Ma, SQM 2021

7

CME measured in Au+Au collisions

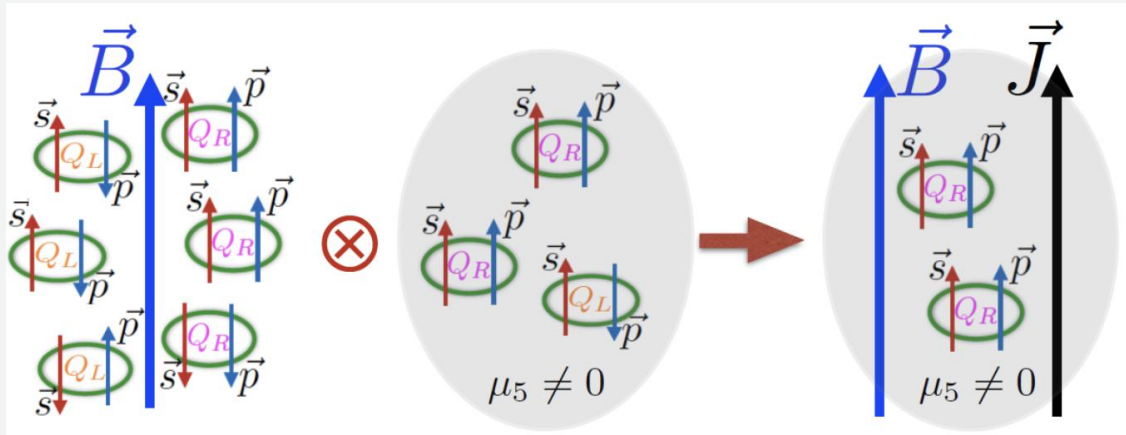


H. Xu, et.al, CPC42, 084103 (2018)

STAR, arXiv:2106.09243

III. 核结构对手征磁效应测量的影响

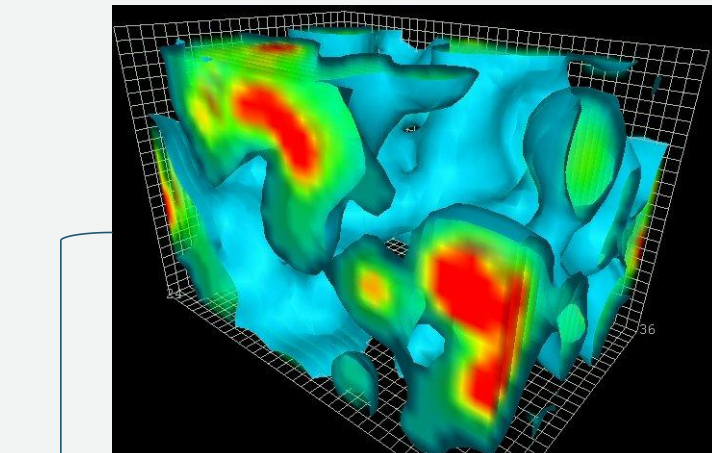
Chiral magnetic effect



Chiral magnetic effect (CME)

$$\mathbf{J}_{\text{cme}} = \sigma_5 \mathbf{B} = \left(\frac{(Qe)^2}{2\pi^2} \mu_5 \right) \mathbf{B},$$

D. Kharzeev, PPNP88, 1(2016)

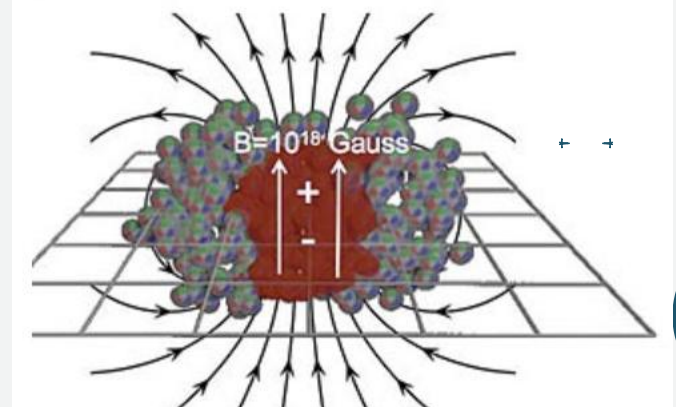


QCD Vacuum:
Fluctuations of
topological
charge

$$Q_w = \frac{g^2}{32\pi^2} \int d^4x F_{\mu\nu}^a \tilde{F}_a^{\mu\nu}$$

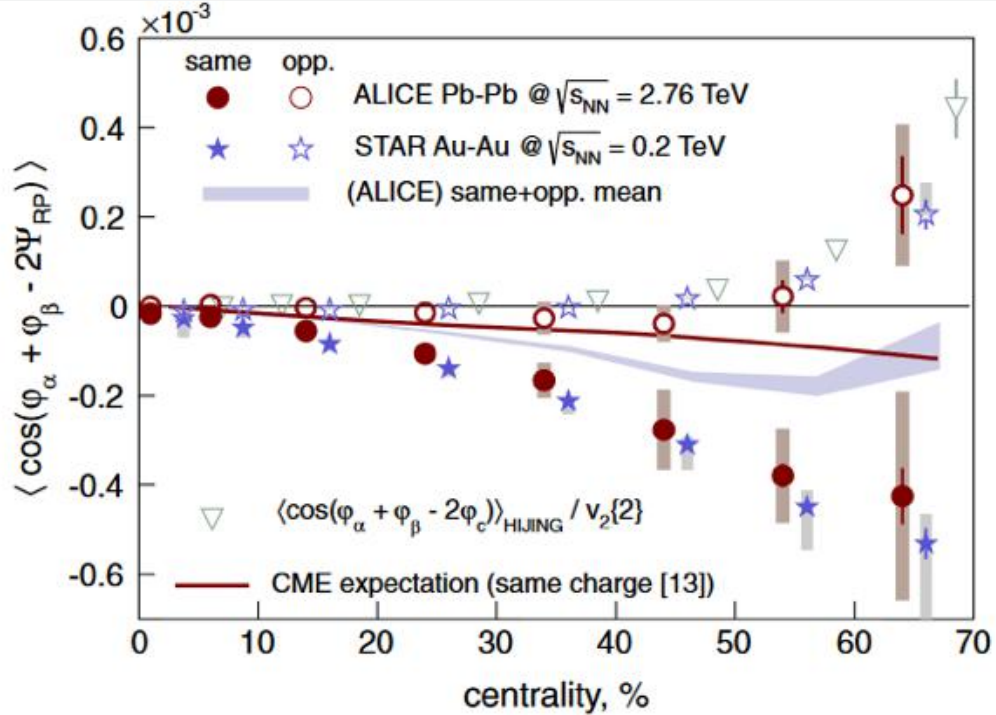
Strong magnetic
field

$$eB \sim m_\pi^2 @ HIC$$



Signal and v_2 background

$$\gamma \equiv \langle \cos(\varphi_\alpha + \varphi_\beta - 2\Psi_{RP}) \rangle$$



STAR, PRL103, 251601 (2009)

ALICE, PRL110, 012301 (2013)

$$y(B)$$

$$\pi^+ \pi^-$$

$$\pi^+$$

$$\rho$$

$$\pi^-$$

$$\rho$$

$$\rho$$

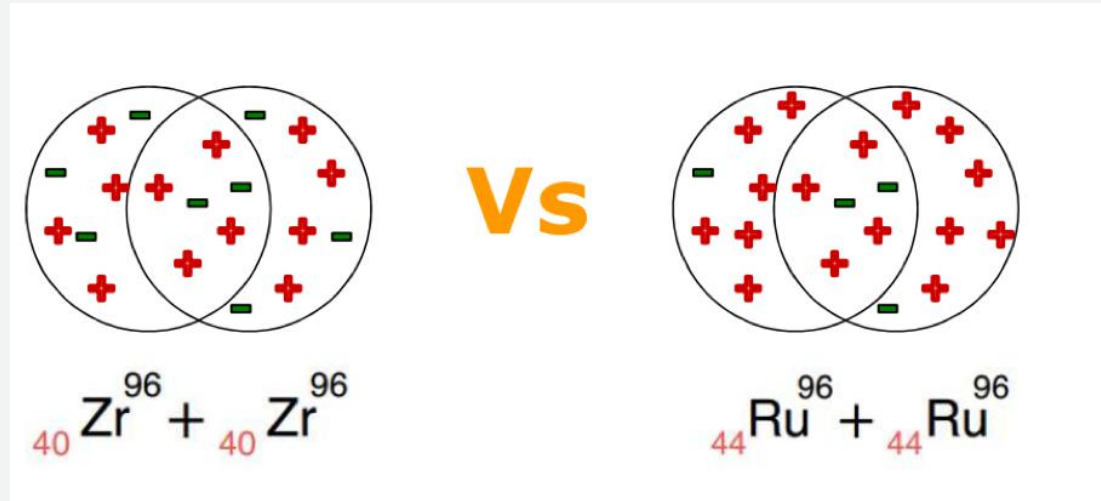
$$\rho$$

$$\pi^+$$

$$\pi^-$$

$$\$$

Isobar collisions

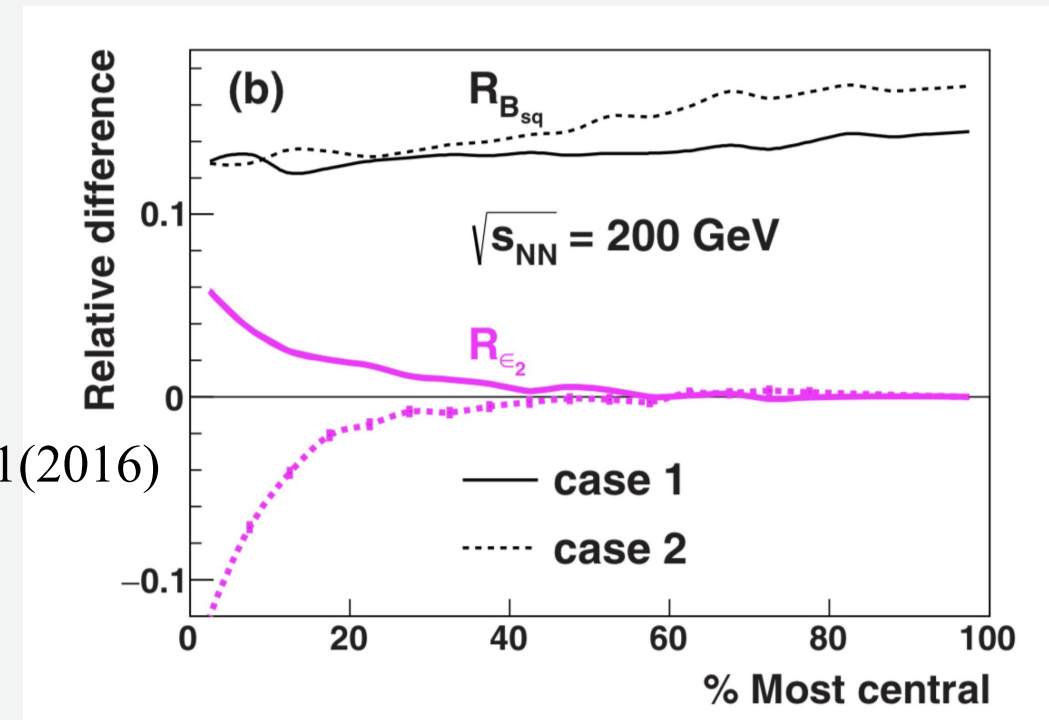


W. Deng, X. Huang, PRC94, 041901(2016)

	R	a	β_2
Zr	5.02	0.46	0.08/0.217
Ru	5.085	0.46	0.158/0.053

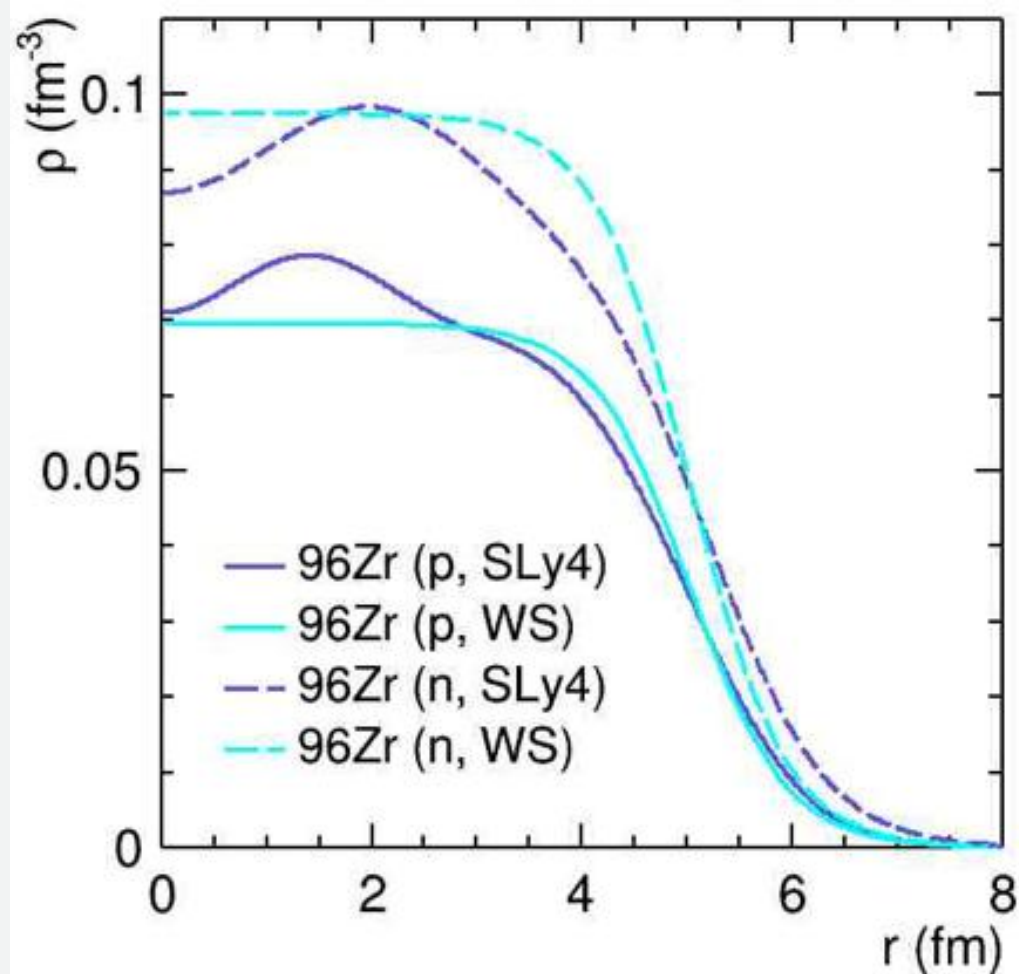
徐浩浩, 湖州师范学院

The isobar collisions was proposed to measure the **chiral magnetic effect**.
S. Voloshin, PRL105, 172301 (2010)

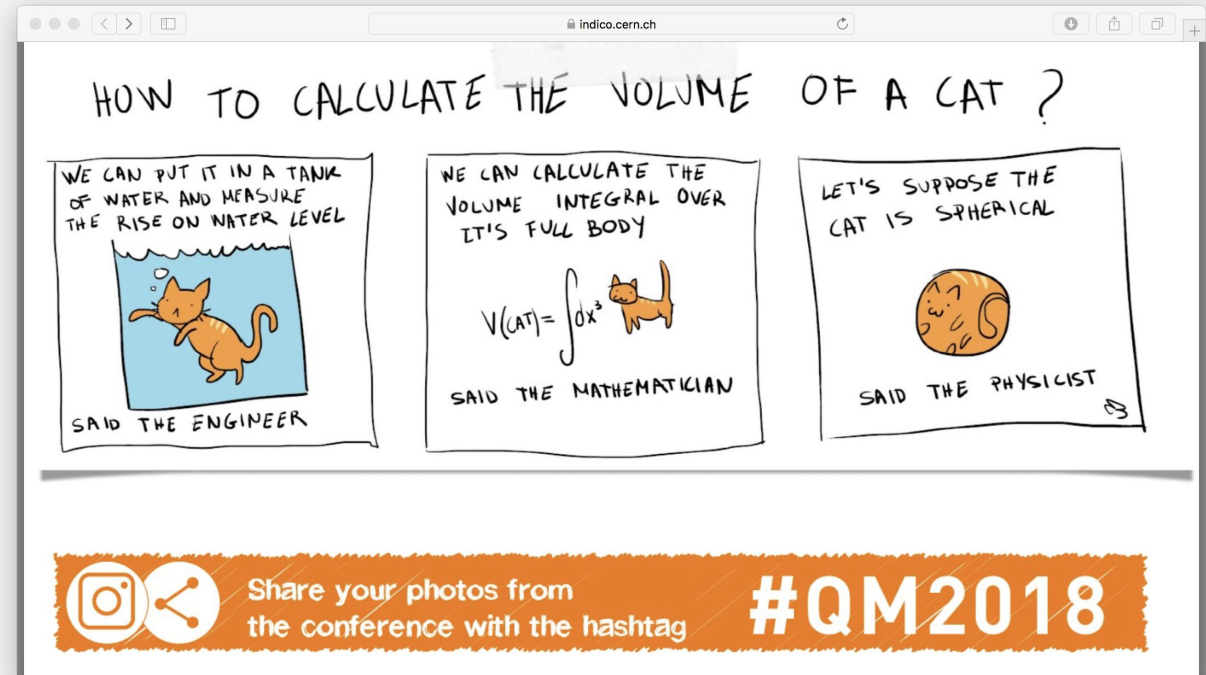


- Same eccentricities => flow background
- Different magnetic field => CME signals

DFT densities VS WS densities

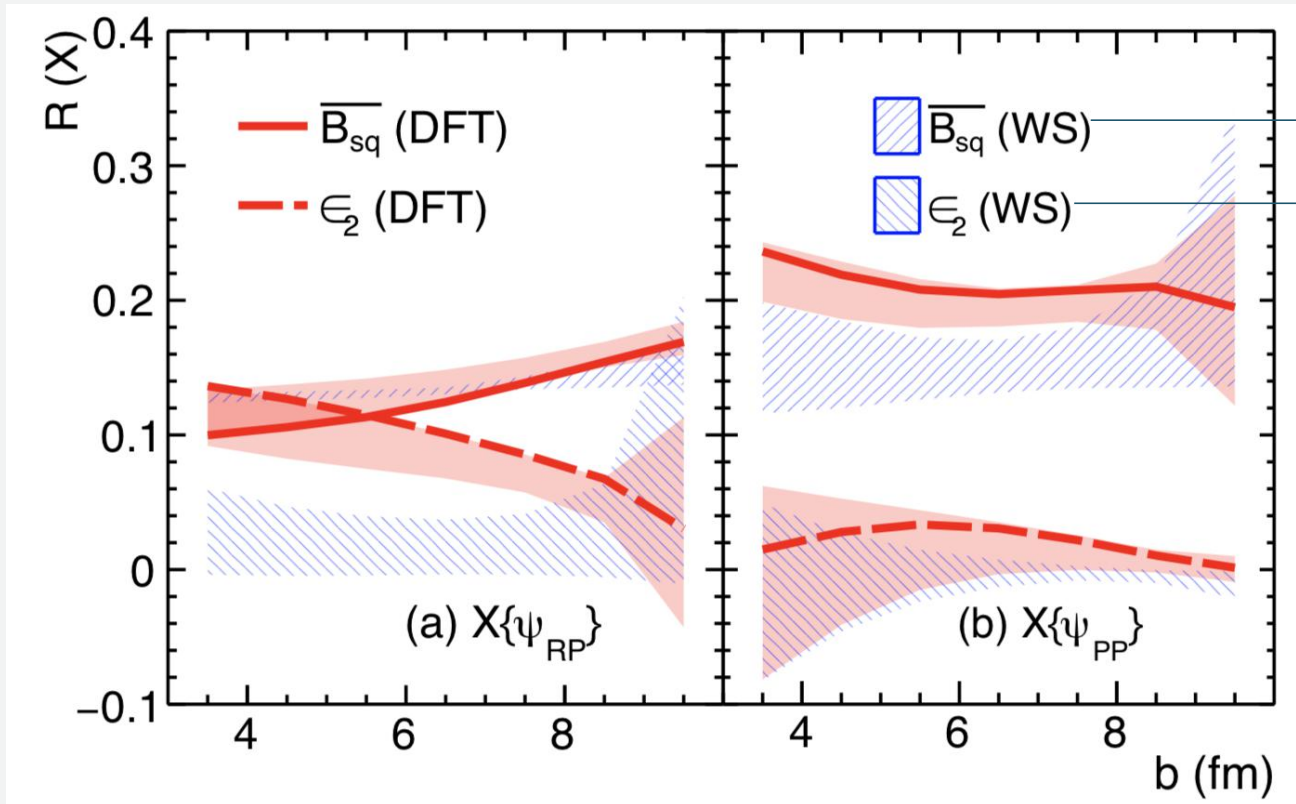


H. Xu, et.al, PRL121, 022301 (2018)



Instead of the WS densities, we use the densities obtained from the **density functional theory (DFT)** with parameter set SLy4.

Static model: Monte Carlo Glauber model



Signal
Background

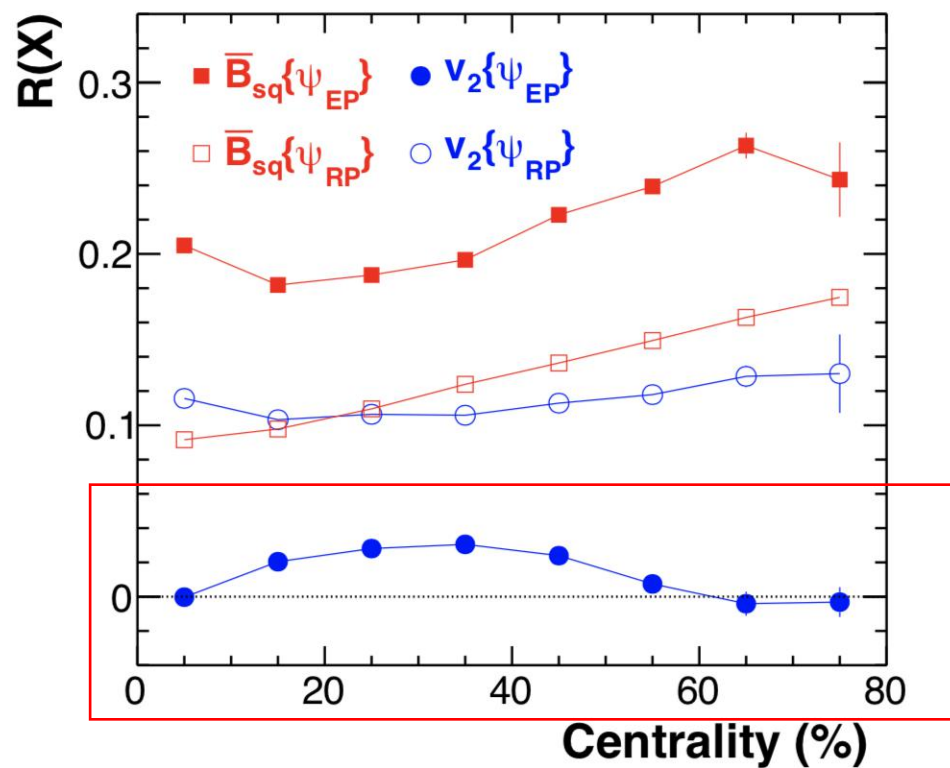
Monte Carlo Glauber Model

$$R(X) \equiv 2(X_{\text{RuRu}} - X_{\text{ZrZr}})/(X_{\text{RuRu}} + X_{\text{ZrZr}}),$$

$$\epsilon_2\{\psi\} = \langle \langle \cos 2(\phi - \psi) \rangle \rangle$$

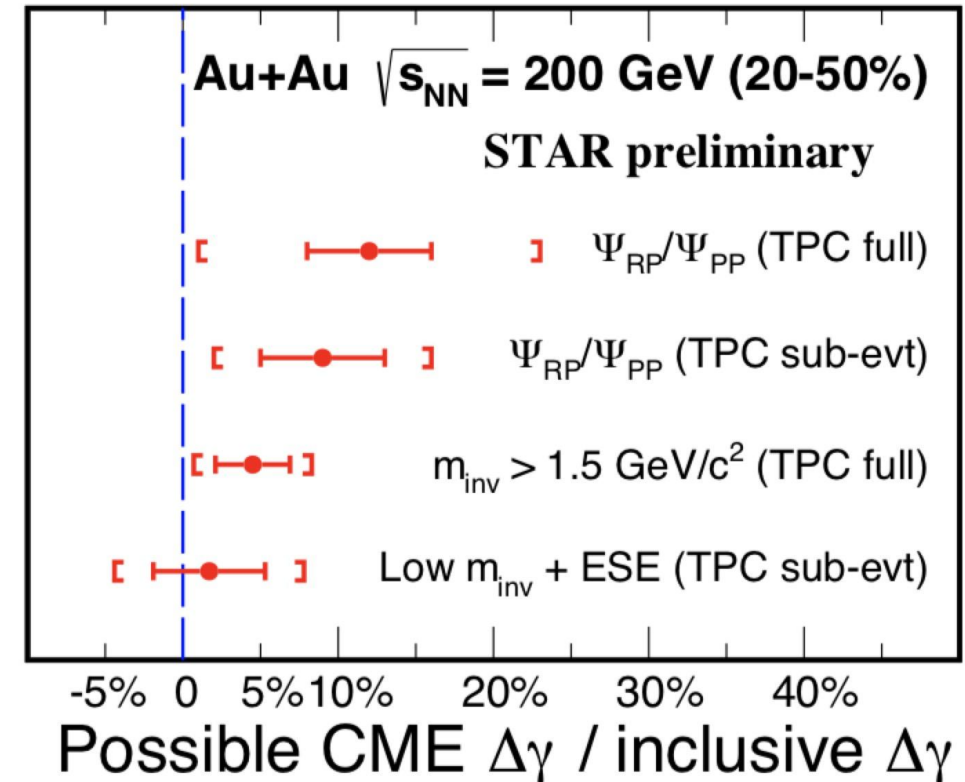
$$\overline{B_{sq}}\{\psi\} = \left\langle \int N_{part}^2(\mathbf{r}) (eB(r, 0)/m_\pi^2)^2 \cos 2(\psi_B - \psi) d\mathbf{r} / \int N_{part}^2(\mathbf{r}) d\mathbf{r} \right\rangle$$

AMPT simulations



AMPT model

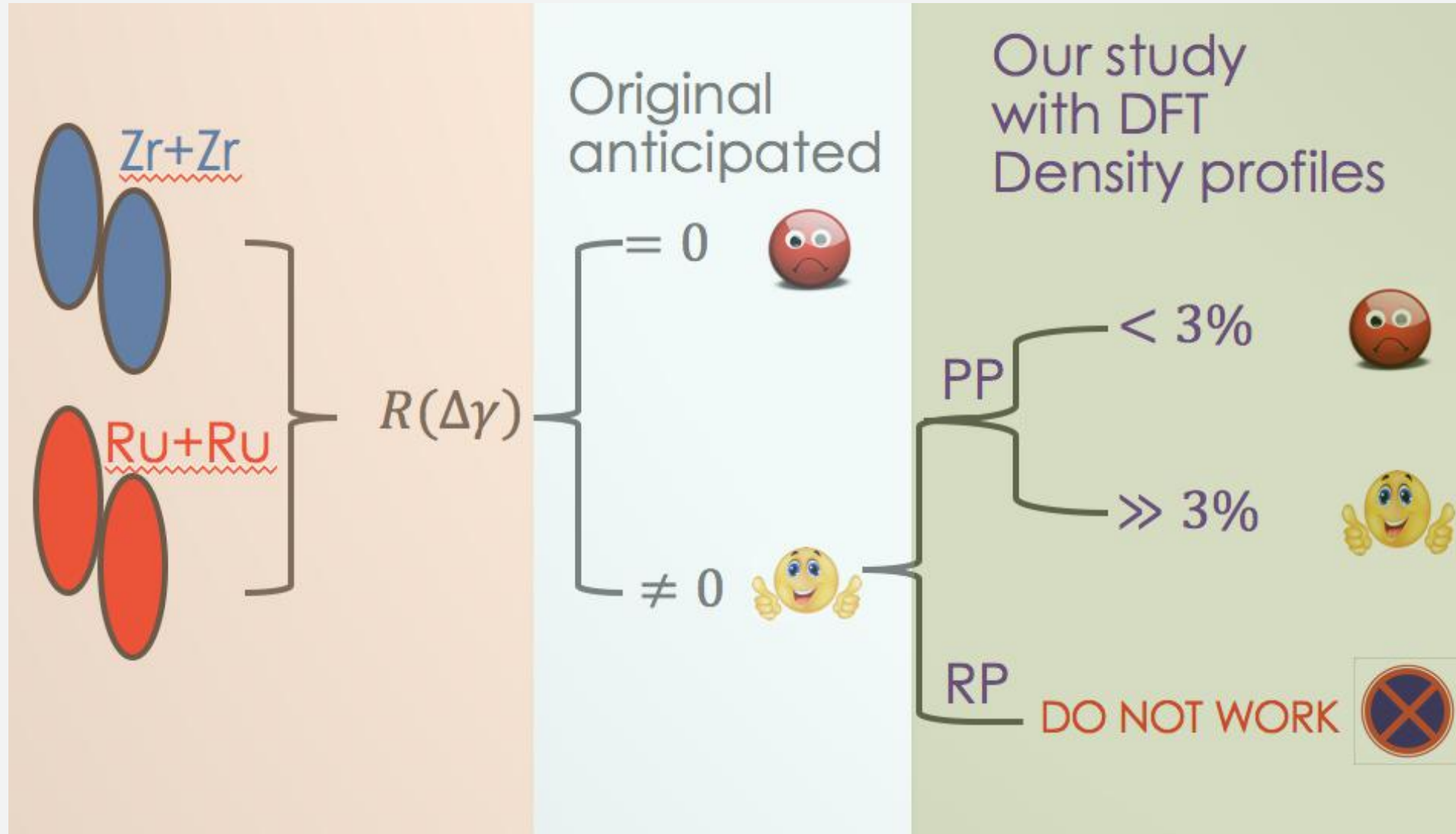
徐浩洁, 湖州师范学院



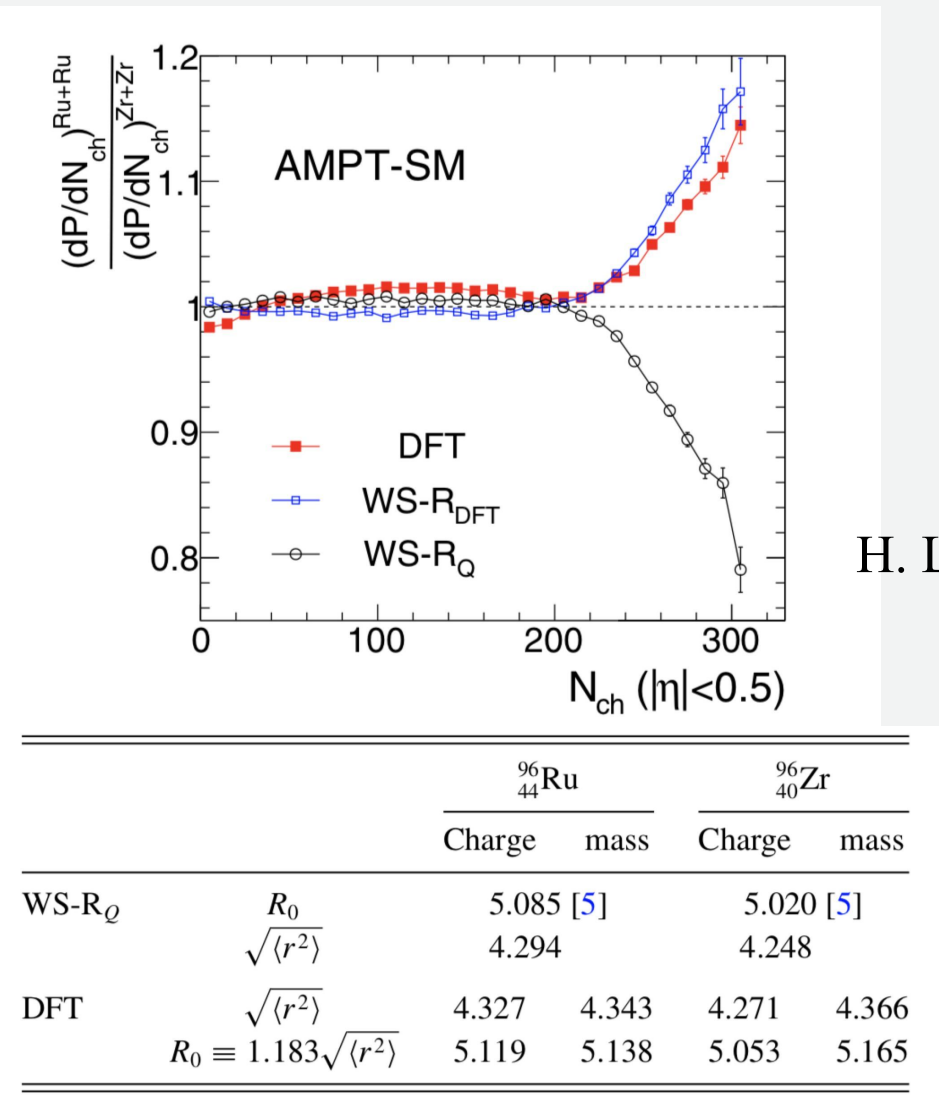
J. Zhao (STAR), NPA982, 535(2019)

Background dominated

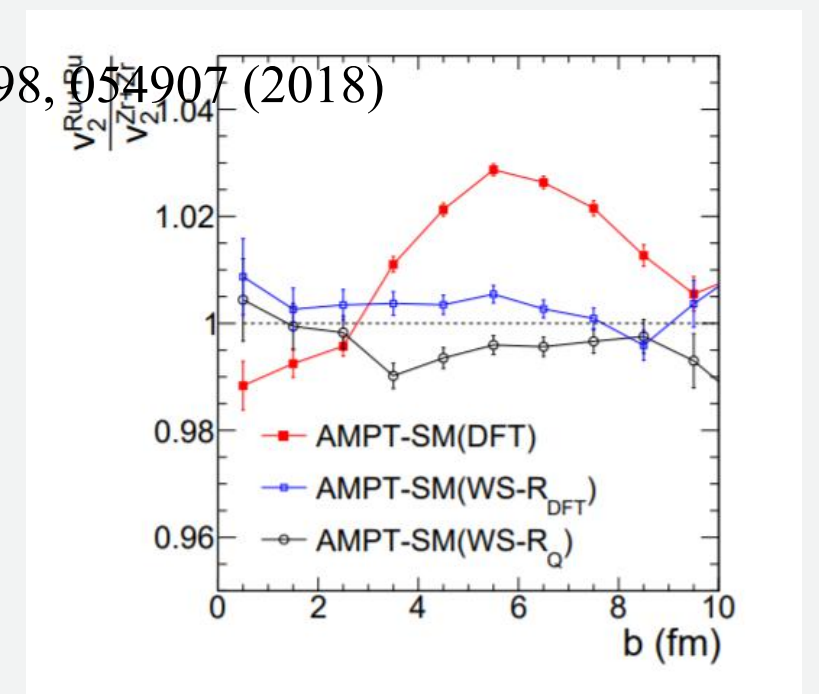
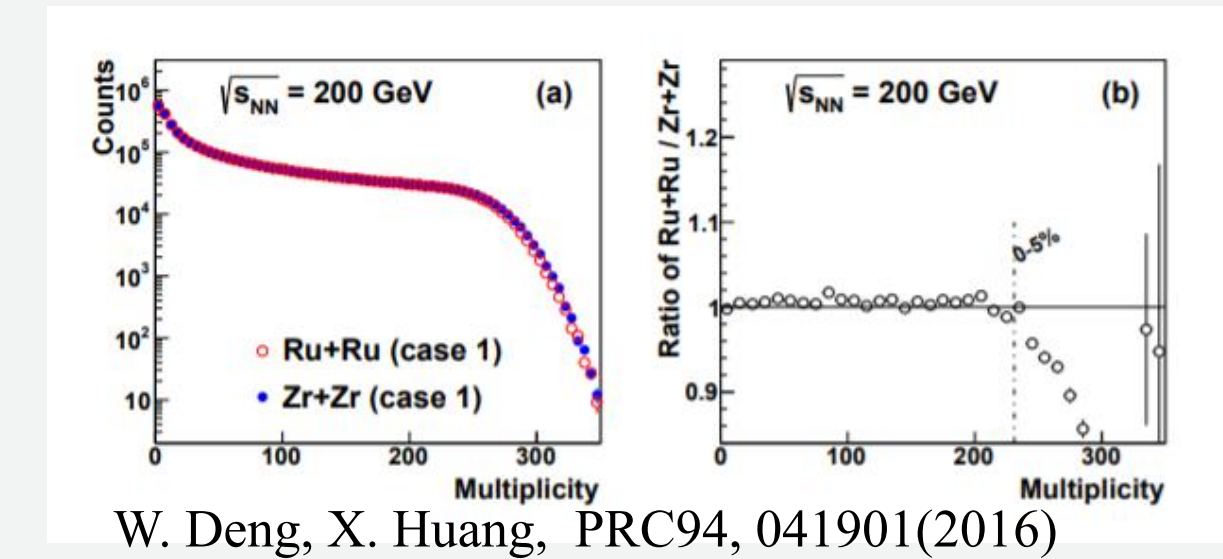
--- The CME signal, if exist, is very small



Multiplicity distributions



徐浩洁，湖州师范学院



IV. 通过同量异位素核碰撞测量中子皮

Neutron skin from antiprotonic atoms

VOLUME 87, NUMBER 8

PHYSICAL REVIEW LETTERS

20 AUGUST 2001

Neutron Density Distributions Deduced from Antiprotonic Atoms

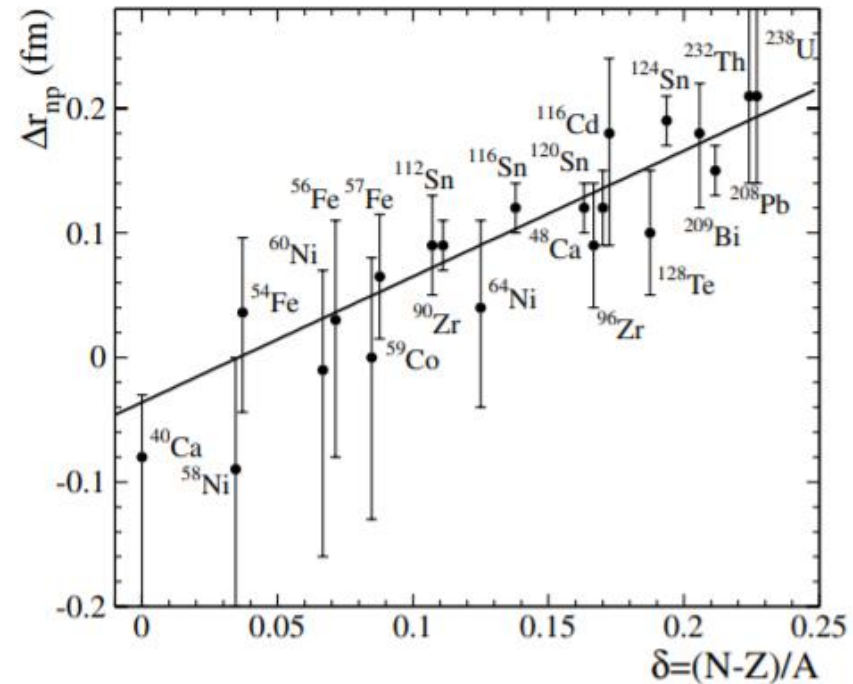
A. Trzcińska, J. Jastrzębski, and P. Lubiński

Heavy Ion Laboratory, Warsaw University, PL-02-093 Warsaw, Poland

F.J. Hartmann, R. Schmidt, and T. von Egidy

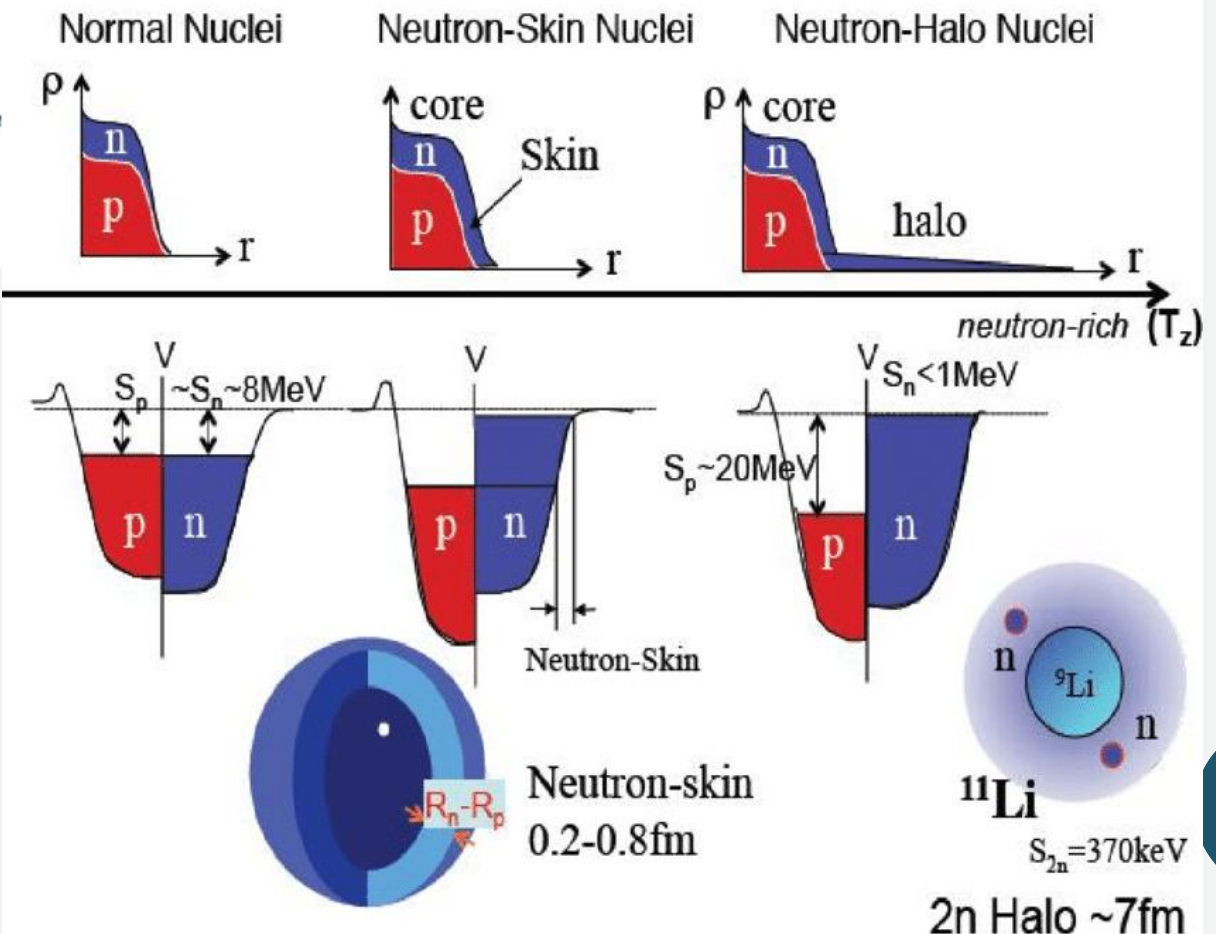
Physik-Department, Technische Universität München, D-85747 Garching, Germ

B. Kłos



徐浩洁，湖州师范学院

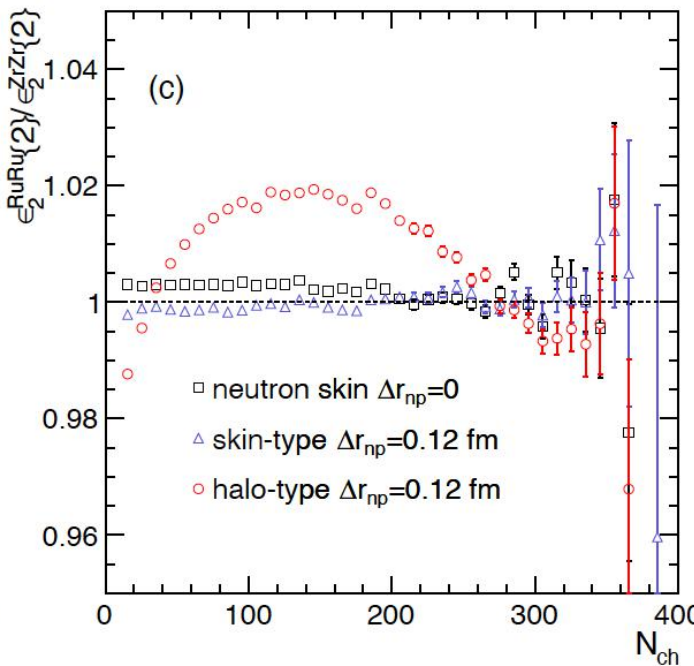
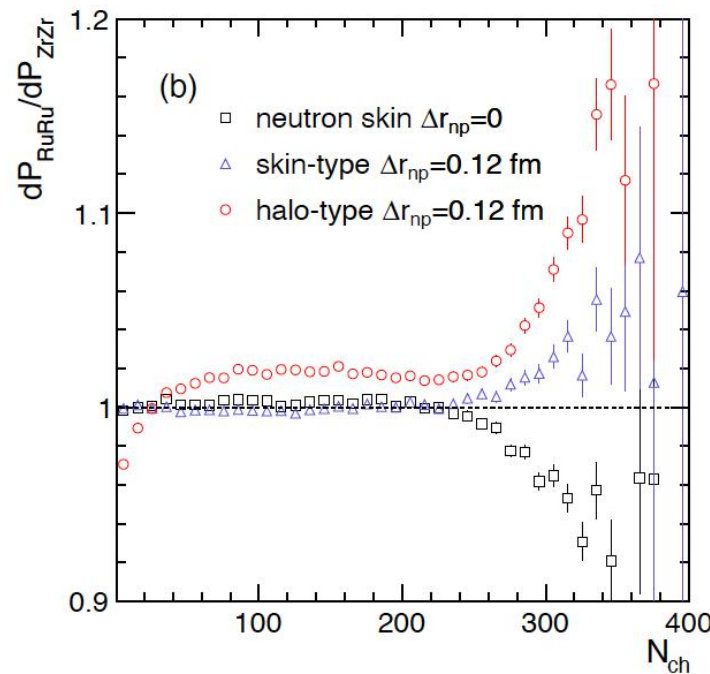
Katowice, Poland
(August 2001)



Determine the neutron skin type

H. Xu, H. Li, X. Wang, C. Shen, F. Wang,
PLB819, 136453 (2021)

	⁹⁶ Ru		⁹⁶ Zr	
	<i>R</i>	<i>a</i>	<i>R</i>	<i>a</i>
p	5.085	0.523	5.021	0.523
skin-type n	5.085	0.523	5.194	0.523
halo-type n	5.085	0.523	5.021	0.592



- The N_{ch} ratios bends up above unity at large N_{ch} because the larger neutron skin thickness of Zr
- The shapes of the Ru+Ru/Zr+Zr ratios of the N_{ch} distributions and eccentricity in mid-central collisions can further distinguish between skin-type and halo-type neutron densities, both having the same skin thickness.

Nuclear density distributions

SHF: Standard Skyrme-Hartree-Fock (SHF) model

eSHF: Extended SHF model

$$E(\rho, \delta) = E_0(\rho) + E_{sym}(\rho)\delta^2 + O(\delta^4)$$

$$\rho = \rho_n + \rho_p; \quad \delta = \frac{\rho_n - \rho_p}{\rho}; \quad \rho_c \simeq 0.11 fm^{-3}$$

$$L(\rho_c) = 3\rho_c \left[\frac{dE_{sym}(\rho)}{d\rho} \right]_{\rho=\rho_c}$$

Z. Zhang, PRC94, 064326(2016)

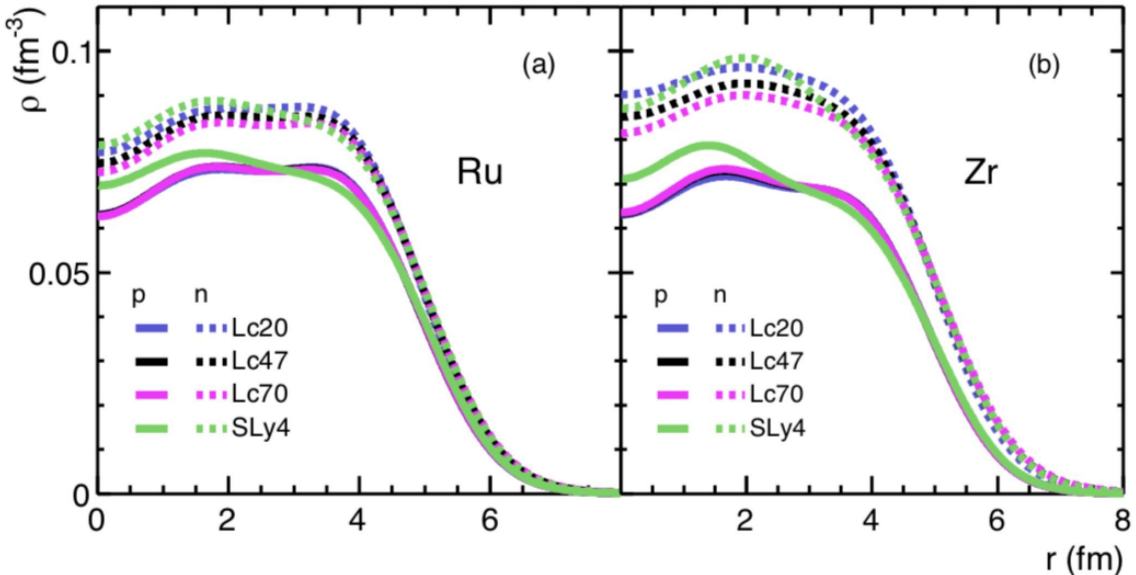
$$\begin{aligned}
 v_{i,j} &= t_0(1 + x_0 P_\sigma) \delta(\mathbf{r}) + \frac{1}{6} t_3(1 + x_3 P_\sigma) \rho^\alpha(\mathbf{R}) \delta(\mathbf{r}) \\
 &+ \frac{1}{2} t_1(1 + x_1 P_\sigma) [K'^2 \delta(\mathbf{r}) + \delta(\mathbf{r}) K^2] \\
 &+ t_2(1 + x_2 P_\sigma) \mathbf{K}' \cdot \delta(\mathbf{r}) \mathbf{K} \\
 &+ \frac{1}{2} t_4(1 + x_4 P_\sigma) [K'^2 \delta(\mathbf{r}) \rho(\mathbf{R}) + \rho(\mathbf{R}) \delta(\mathbf{r}) K^2] \\
 &+ t_5(1 + x_5 P_\sigma) \mathbf{K}' \cdot \rho(\mathbf{R}) \delta(\mathbf{r}) \mathbf{K} \quad \text{Extended} \\
 &+ iW_0(\boldsymbol{\sigma}_i + \boldsymbol{\sigma}_j) \cdot [\mathbf{K}' \times \delta(\mathbf{r}) \mathbf{K}],
 \end{aligned}$$

(4)

	eSHF	SHF								
$L(\rho_c)$ (MeV)	20.000	47.300	70.000	42.661						
$E_{sym}(\rho_c)$ (MeV)	26.650	26.650	26.650	26.450						
ρ_0 (fm ⁻³)	0.15414	0.15267	0.15059	0.15954						
t_0 (MeV · fm ³)	-2063.0	-2037.3	-1855.3	-2488.9						
t_1 (MeV · fm ⁵)	442.48	524.18	576.91	486.82						
t_2 (MeV · fm ⁵)	-562.02	-521.60	-76.702	-54.640						
t_3 (MeV · fm ^{3+3\alpha})	14726.	13734.	12367.	13777.						
t_4 (MeV · fm ^{5+3\beta})	-1532.5	-1615.7	-1650.2	-						
t_5 (MeV · fm ^{5+3\gamma})	3037.5	2153.2	-436.51	-						
x_0	0.92728	0.29070	-0.26752	0.83400						
x_1		1.3163	0.37275	-0.51268	-0.34400					
x_2			-0.55463	-0.55121	3.1558	-1.00000				
x_3				0.98695	0.13143	-0.83906	1.35400			
x_4					1.7600	0.29499	-1.5709	-		
x_5						-0.83852	-0.65206	-4.1683	-	
α						0.28356	0.27858	0.31853	0.16667	
β							1	1	1	-
γ								1	1	-
W_0 (MeV · fm ⁵)	92.759	100.14	113.61	123.00						

Additional density-dependent two-body forces to effectively simulate the momentum-dependent three-body forces

Neutron skin thickness

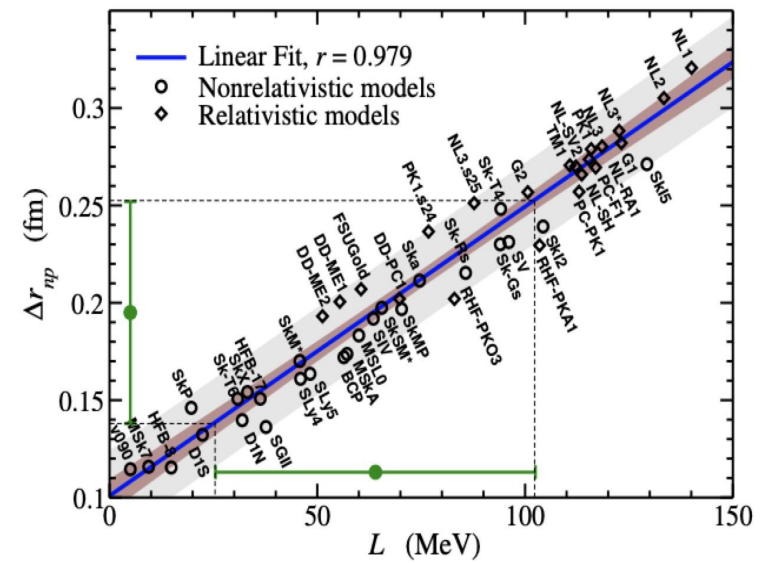


$$\sqrt{\langle r^2 \rangle} = \sqrt{\int \rho(r) r^4 dr / \int \rho(r) r^2 dr}$$

$$\Delta r_{np} = r_n - r_p$$

The four interactions give **similar proton rms**, but the **neutron radius increase with $L(\rho_c)$**

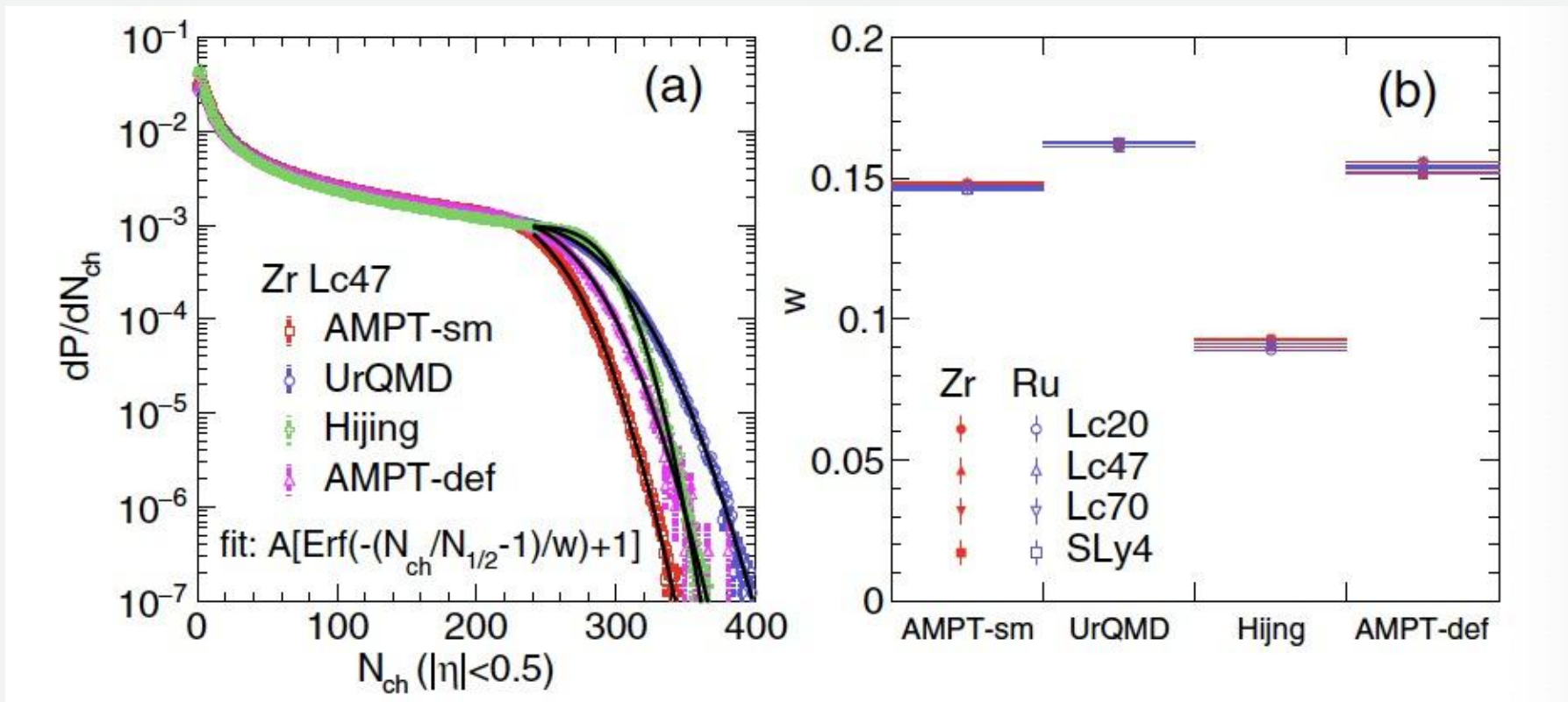
	$L(\rho_c)$	$L(\rho_0)$	⁹⁶ Zr			⁹⁶ Ru			²⁰⁸ Pb
			r_n	r_p	Δr_{np}	r_n	r_p	Δr_{np}	Δr_{np}
Lc20	20	13.1	4.386	4.27	0.115	4.327	4.316	0.011	0.109
Lc47	47.3	55.7	4.449	4.267	0.183	4.360	4.319	0.042	0.190
Lc70	70	90.0	4.494	4.262	0.232	4.385	4.32	0.066	0.264
SLy4	42.7	46.0	4.432	4.271	0.161	4.356	4.327	0.030	0.160



Heavy ion event generators

- Heavy ion jet interaction generator (Hijing)
- A Multi-Phase Transport model (AMPT)
 - Default (String fragmentation)
 - String melting
- Ultra relativistic Quantum Molecular Dynamics (UrQMD)

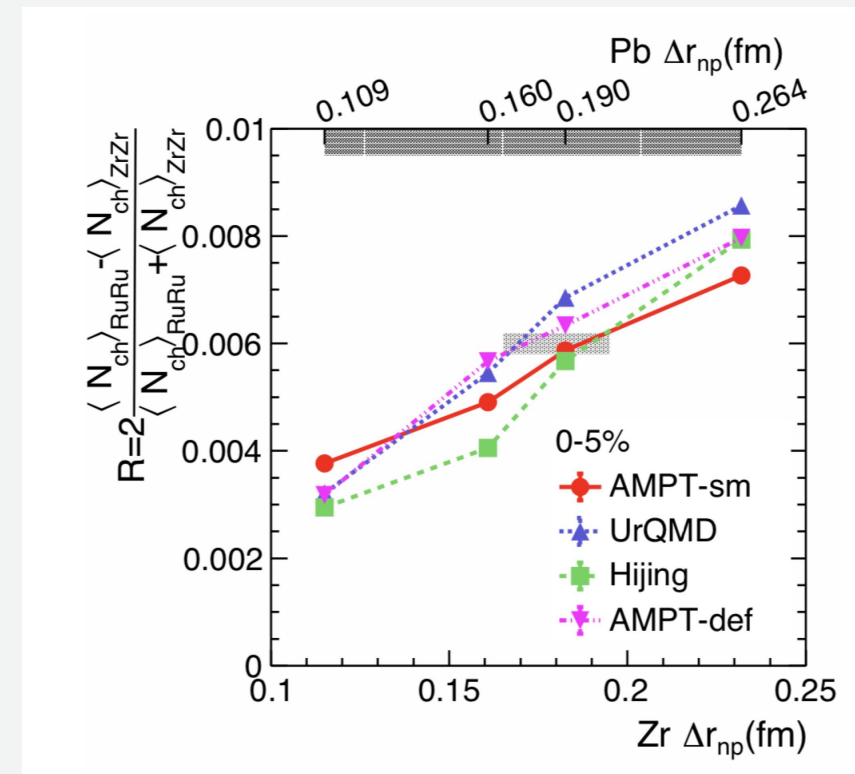
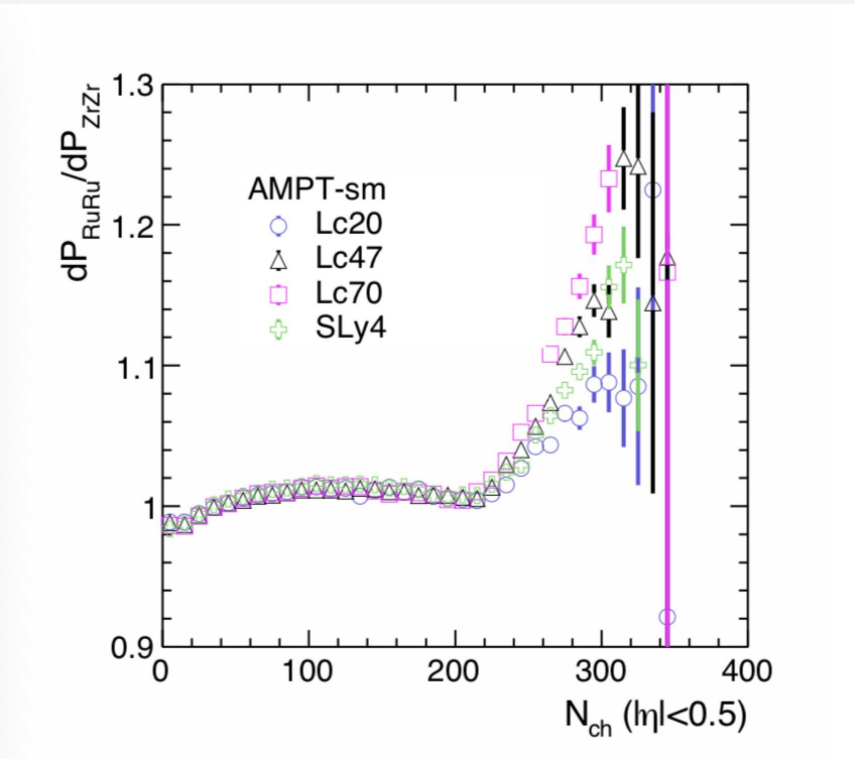
Multiplicity distributions



$$dP/dN_{ch} \propto -\text{Erf}[-(N_{ch}/N_{1/2} - 1)/w] + 1, \quad (1)$$

The effect is **hardly observable** in a plot of the N_{ch} distributions themselves.

Ratios of N_{ch} distributions



- The ratio of N_{ch} distributions **highlight the differences** but cumbersome to quantify
- To **quantify the differences**, we use **the R observable** of $\langle N_{ch} \rangle$ at top 5% centrality.

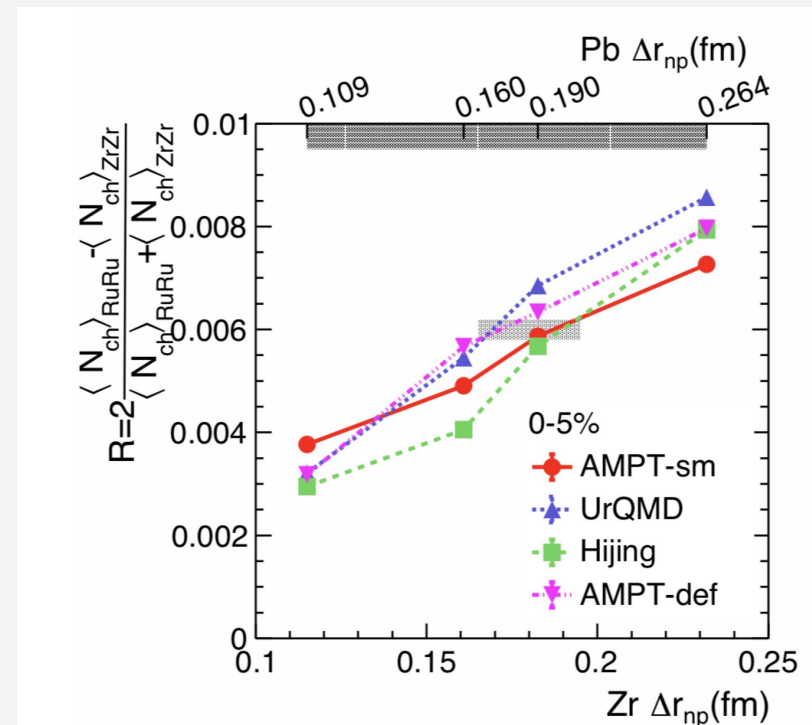
The R observable

R is a relative measure, **much of experimental effects cancel:**

1. **Track inefficiency:** We use only 0-5% central collisions , where the tracking efficiency is constant to a good degree
2. **Trigger inefficiency:** the trigger inefficiency can be corrected in experiment. Even without correction, the uncertainty is about 2×10^{-4} , negligible small.

Question: The R observable is actually an isospin insensitive observable, why it have **rather weak model dependence?**

The particle production in relativistic heavy ion collisions **is insensitive to the details of the QCD physics**, which is in contrast to the hadronic observables in low-energy studies.



初态几何模型

- **Glauber model**

$$\frac{dN}{dy} \propto s \propto \frac{(1-x)}{2} n_{part} + xn_{coll}$$

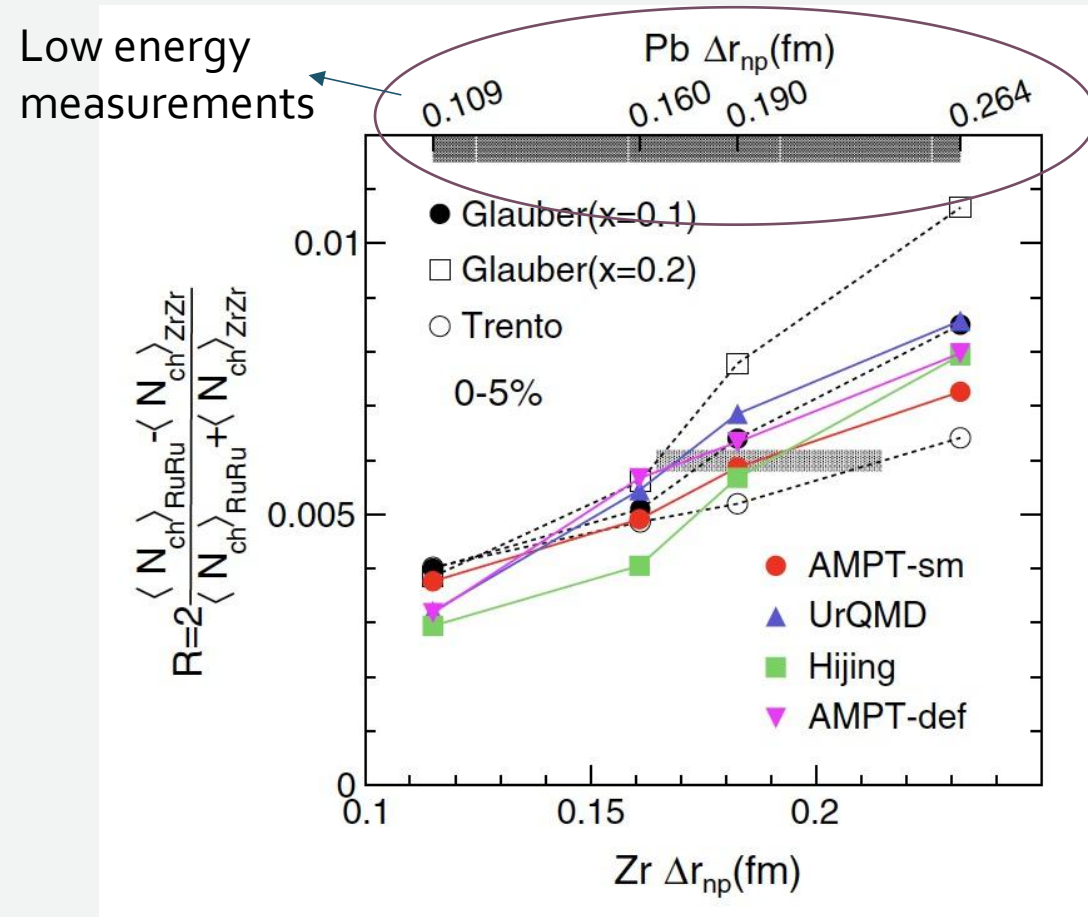
n_{part} : number of participant; n_{coll} : number of binary collisions

$x = 0.1$ (default), $x = 0.2$ (extreme)

- **Trento model** (J. Moreland, et.al, PRC92, 011901(2015))

$$\frac{dN}{dy} \propto s \propto \left(\frac{T_A^p + T_B^p}{2}\right)^{1/p}; p = 0 \text{ and } k = 1.4$$

Probe the neutron skin thickness



The **R observable** in isobaric collisions at ultra-relativistic energies provide a novel approach to **determine the neutron skin thickness** to a precision that may comparable to or even exceed those achieved by traditional **low-energy nuclear experiments**.

STAR isobar collisions (2018):

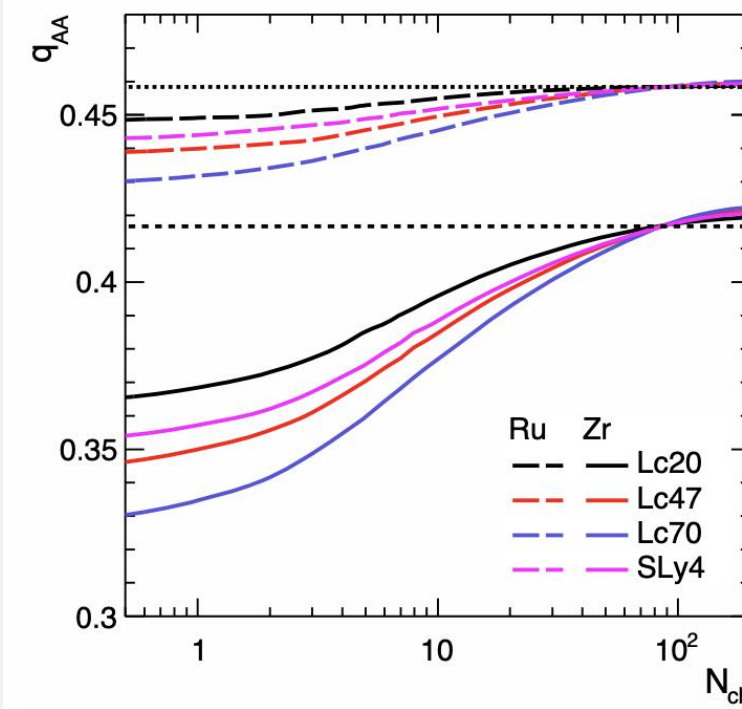
- **More statistics:** 6.3 billion isobar events
- **Less systematical uncertainty**

4 **dynamic** models + 2 **static** models

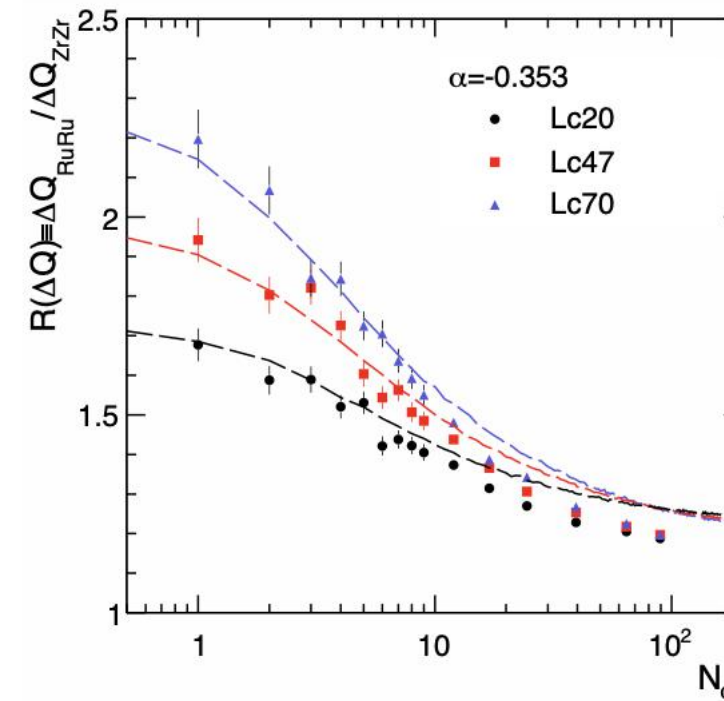
Grazing isobaric collisions

H. Xu, H. Li, Y. Zhou, X. Wang, J. Zhao, L. Chen, F. Wang,
arXiv:2105.04052 (2021)

Number of participant protons /
Number of total participants



Net charge number ratios
between Ru+Ru and Zr+Zr



superimposition
assumption

$$\Delta Q_{AA} \propto q_{AA} \Delta Q_{pp} + (1 - q_{AA}) \Delta Q_{nn},$$

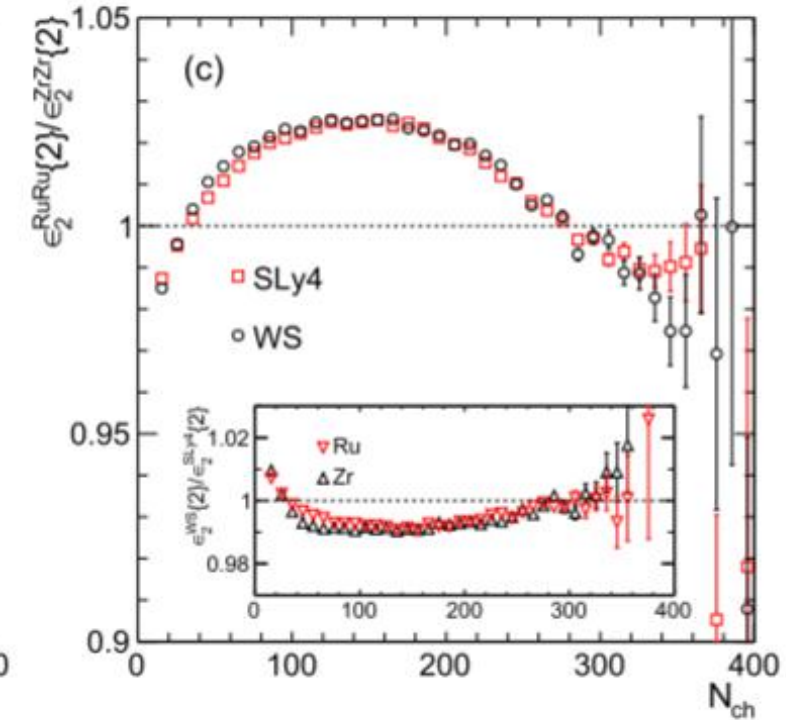
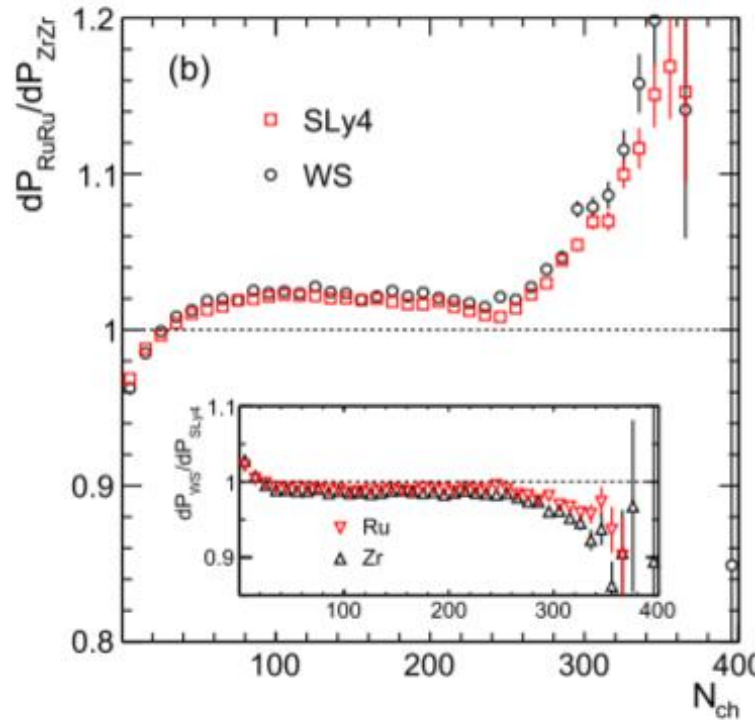
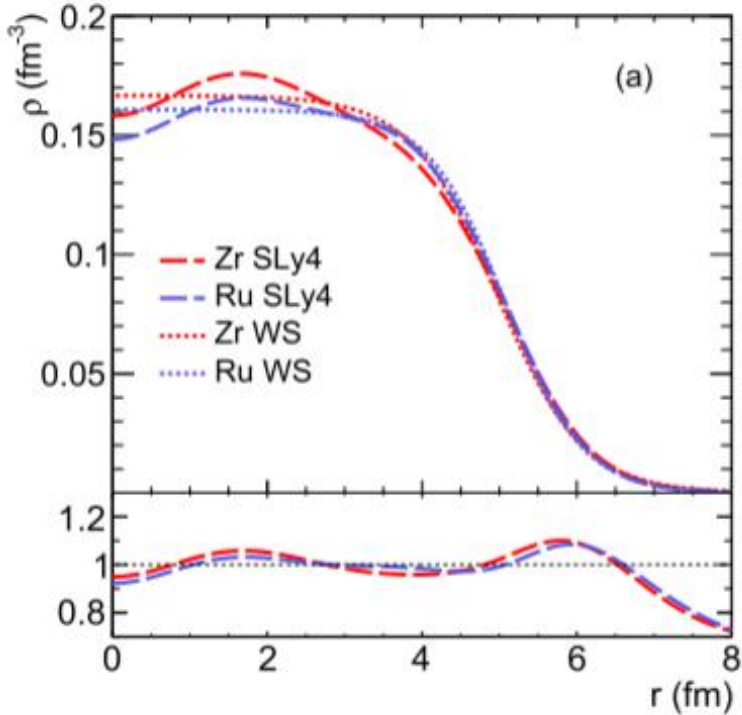
$$R_{\Delta Q} \equiv \frac{\Delta Q_{\text{RuRu}}}{\Delta Q_{\text{ZrZr}}} = \frac{q_{\text{RuRu}} + \alpha/(1-\alpha)}{q_{\text{ZrZr}} + \alpha/(1-\alpha)},$$

UrQMD model
Trento model

We propose a direct measurement of the neutron skin by using net-charge multiplicities in ultra-peripheral (grazing) collisions of those isobars.

DFT and WS densities

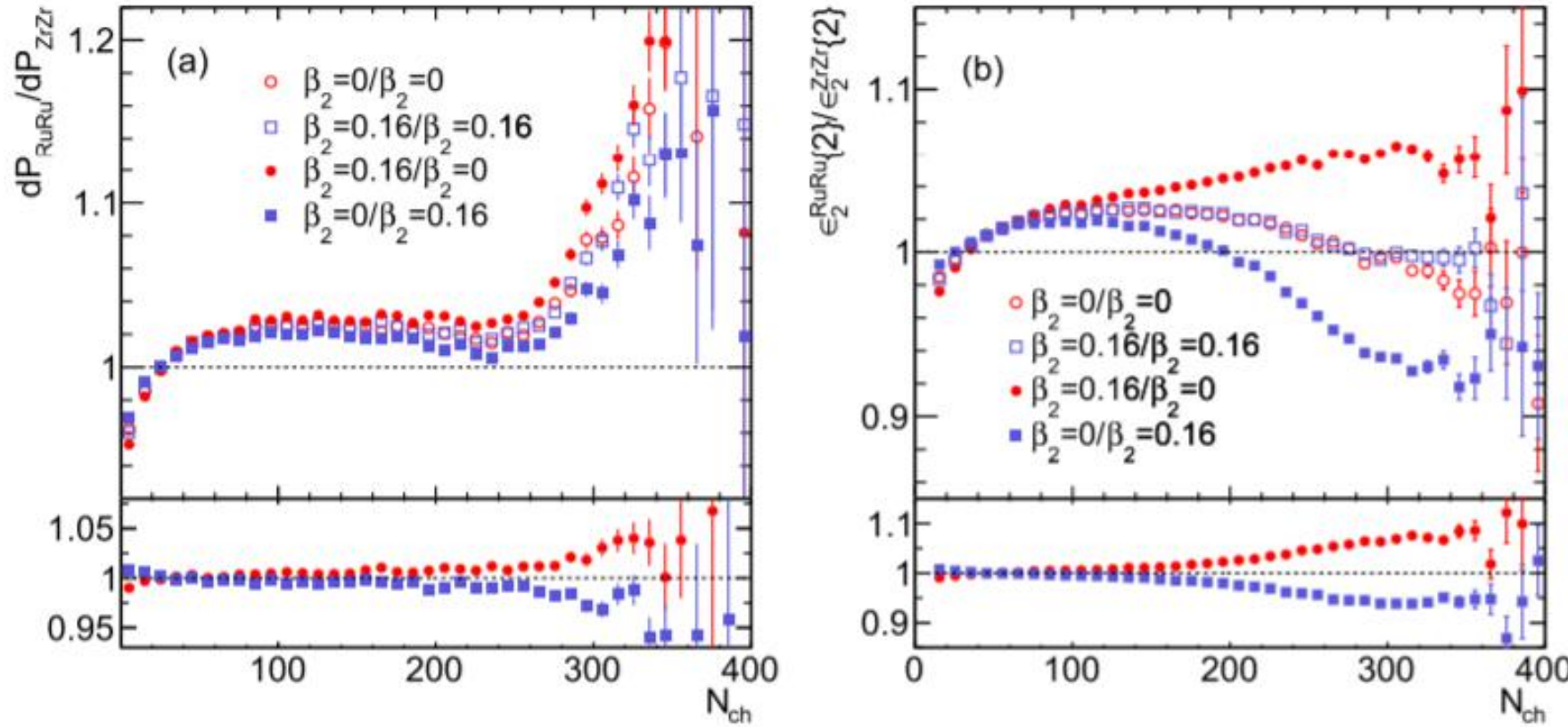
H. Xu, H. Li, X. Wang, C. Shen, F. Wang,
PLB819, 136453 (2021)



$$\langle r \rangle_{\text{DFT}} = \langle r \rangle_{\text{WS}}$$
$$\langle r^2 \rangle_{\text{DFT}} = \langle r^2 \rangle_{\text{WS}}$$

Effective of nuclei deformation

H. Xu, H. Li, X. Wang, C. Shen, F. Wang,
PLB819, 136453 (2021)



Giuliano Giacalone, Jiangyong Jia, Vittorio Soma, arXiv:2102.08158
Giuliano Giacalone, Jiangyong Jia, Chunjian Zhang, arXiv: 2105.01638
Jiangyong Jia, Shenli Huang, Chunjiang Zhang, arXiv:2105.05713
Jiangyong Jia, arXiv:2106.08768

V 总结

PHYSICAL REVIEW LETTERS 125, 222301 (2020)

arXiv: 1910.06170

Probing the Neutron Skin with Ultrarelativistic Isobaric Collisions

Hanlin Li¹, Hao-jie Xu^{2,*}, Ying Zhou,³ Xiaobao Wang,² Jie Zhao,⁴ Lie-Wen Chen,^{3,†} and Fuqiang Wang^{2,4,‡}

¹College of Science, Wuhan University of Science and Technology, Wuhan, Hubei 430065, China

²School of Science, Huzhou University, Huzhou, Zhejiang 313000, China

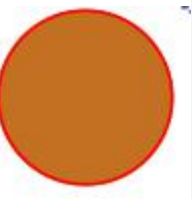
³School of Physics and Astronomy and Shanghai Key Laboratory for Particle Physics and Cosmology, Shanghai Jiao Tong University, Shanghai 200240, China

⁴Department of Physics and Astronomy, Purdue University, West Lafayette, Indiana 47907, USA

(Received 24 October 2019; accepted 15 October 2020; published 23 November 2020)

Particle production in ultrarelativistic heavy ion collisions depends on the details of the nucleon density distributions in the colliding nuclei. We demonstrate that the charged hadron multiplicity distribution in isobaric collisions at ultrarelativistic energies provide a novel approach to determine the poorly known neutron density distributions and thus the neutron skin thickness in finite nuclei, which can in turn stringent constraints on the nuclear symmetry energy.

DOI: 10.1103/PhysRevLett.125.222301



May 2021

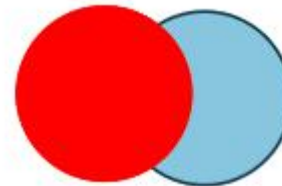
Physics Letters B 819 (2021) 136453



Contents lists available at ScienceDirect

Physics Letters B

www.elsevier.com/locate/physletb



Determine the neutron skin type by relativistic isobaric collisions

Hao-jie Xu^{a,*}, Hanlin Li^b, Xiaobao Wang^a, Caiwan Shen^a, Fuqiang Wang^{a,c,*}



^a School of Science, Huzhou University, Huzhou, Zhejiang 313000, China

^b College of Science, Wuhan University of Science and Technology, Wuhan, Hubei 430065, China

^c Department of Physics and Astronomy, Purdue University, West Lafayette, IN 47907, USA

arXiv: 2103.05595

ARTICLE INFO

Article history:

Received 17 March 2021

Received in revised form 3 May 2021

Accepted 14 June 2021

Available online 17 June 2021

Editor: D.F. Geesaman

ABSTRACT

The effects of neutron skin on the multiplicity (N_{ch}) and eccentricity (ϵ_2) in relativistic $^{40}_{44}\text{Ru} + ^{96}_{44}\text{Ru}$ and $^{96}_{40}\text{Zr} + ^{96}_{40}\text{Zr}$ collisions at $\sqrt{s_{NN}} = 200$ GeV are investigated with the Trento model. It is found that the Ru+Ru/Zr+Zr ratios of the N_{ch} distributions and ϵ_2 in mid-central collisions are exquisitely sensitive to the neutron skin type (skin vs. halo). The state-of-the-art calculations by energy density functional theory (DFT) favor the halo-type neutron skin and can soon be confronted by experimental data. It is demonstrated that the halo-type density can serve as a good surrogate for the DFT density, and thus can be efficiently employed to probe nuclear deformities by using elliptic flow data in central collisions. We provide hereby a proof-of-principle venue to simultaneously determine the neutron skin type, thickness, and nuclear deformity.

© 2021 The Authors. Published by Elsevier B.V. This is an open access article under the CC BY license (<http://creativecommons.org/licenses/by/4.0/>). Funded by SCOAP³.

Measuring neutron skin by grazing isobaric collisions

Hao-jie Xu^{a,*}, Hanlin Li^{b†}, Ying Zhou,³ Xiaobao Wang,¹ Jie Zhao,⁴ Lie-Wen Chen^{‡,3} and Fuqiang Wang^{§1,4}

¹School of Science, Huzhou University, Huzhou, Zhejiang 313000, China

²College of Science, Wuhan University of Science and Technology, Wuhan, Hubei 430065, China

³School of Physics and Astronomy, Shanghai Key Laboratory for Particle Physics and Cosmology, and Key Laboratory for Particle Astrophysics and Cosmology (MOE),

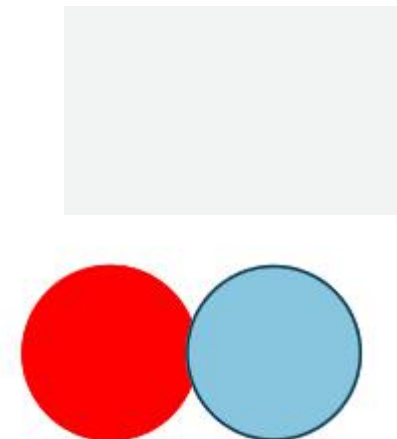
Shanghai Jiao Tong University, Shanghai 200240, China

⁴Department of Physics and Astronomy, Purdue University, West Lafayette, Indiana 47907, USA

Neutron skin thickness (Δr_{np}) of nuclei and the inferred nuclear symmetry energy are of critical importance to nuclear physics and astrophysics. It is traditionally measured by nuclear processes with significant theoretical uncertainties. We recently proposed an indirect measurement of the Δr_{np} by charged hadron multiplicities in central isobaric collisions at relativistic energies, which are sensitive to nuclear densities. In this paper we propose a direct measurement of the Δr_{np} by using net-charge multiplicities in ultra-peripheral (grazing) collisions of those isobars, under the assumption that they are simple superimposition of nucleon-nucleon interactions. We illustrate this novel approach by the TRENTO and URQMD models.

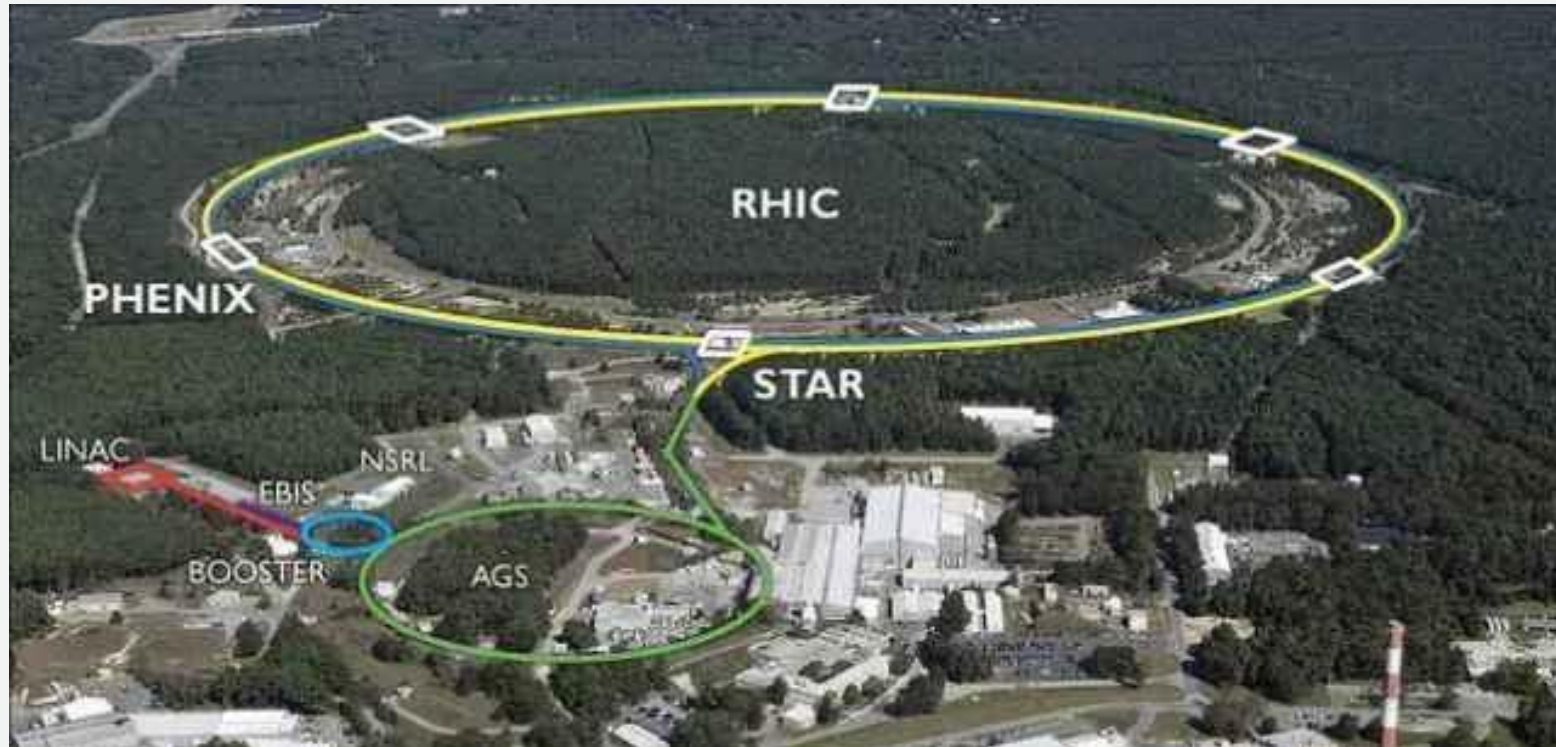
PACS numbers:

arXiv: 2105.04052

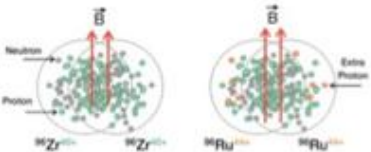


*V*总结

相对论同量异位素核碰撞是研究核结构绝佳平台！



Isobar Blind Analysis



Mock data challenge

Test data structure
(27 GeV files)

Isobar-Mixed Analysis

QA, physics & code freezing
(One run is Ru+Zr)

Isobar-Blind Analysis

Run-by-run QA, full analysis
(One run is Ru/Zr)

Isobar-Unblind Analysis

Full analysis
(Ru and Zr separated)

Processing...

STAR, arXiv:1911.00596
Cartoon: arXiv:2009.01230

Thank you for your attention!